



LUMINOUS INFRARED GALAXIES

D. B. Sanders

[Institute for Astronomy, University of Hawaii](#), 2680 Woodlawn Drive, Honolulu, HI 96822

I. F. Mirabel

Service d'Astrophysique, Centre d'Etudes de Saclay, 91191 Gif sur Yvette, France

KEY WORDS: luminosity function, starbursts, active galactic nuclei, molecular gas, dust emission

ABSTRACT. At luminosities above $10^{11} L_{\odot}$, infrared galaxies become the dominant population of extragalactic objects in the local Universe ($z \lesssim 0.3$), being more numerous than optically selected starburst and Seyfert galaxies and quasi-stellar objects at comparable bolometric luminosity. The trigger for the intense infrared emission appears to be the strong interaction/merger of molecular gas-rich spirals, and the bulk of the infrared luminosity for all but the most luminous objects is due to dust heating from an intense starburst within giant molecular clouds. At the highest luminosities ($L_{\text{ir}} > 10^{12} L_{\odot}$), nearly all objects appear to be advanced mergers powered by a mixture of circumnuclear starburst and active galactic nucleus energy sources, both of which are fueled by an enormous concentration of molecular gas that has been funneled into the merger nucleus. These ultraluminous infrared galaxies may represent an important stage in the formation of quasi-stellar objects and powerful radio galaxies. They may also represent a primary stage in the formation of elliptical galaxy cores, the formation of globular clusters, and the metal enrichment of the intergalactic medium.

Table of Contents

[INTRODUCTION](#)

● [BACKGROUND](#)

- [Pre-IRAS](#)
- [Early IRAS Results](#)

● [REDSHIFT SURVEYS](#)

- [Luminosity Functions](#)
- [Spectral Energy Distributions](#)

● [PROPERTIES OF LUMINOUS INFRARED GALAXIES](#)

- [Optical and Near-Infrared Imaging](#)
- [Optical and Near-Infrared Spectroscopy](#)
- [Mid- and Far-Infrared \(Post-IRAS\) Observations](#)
- [Submillimeter Continuum](#)
- [Radio Continuum](#)
- [Gas Content](#)
- [High-Energy Observations](#)

● [ORIGIN AND EVOLUTION OF LUMINOUS INFRARED GALAXIES](#)

- [Strong Interactions and Mergers](#)
- [Case Studies](#)

● [ASSOCIATED PHENOMENA](#)

- [Formation of Ellipticals](#)
- [Formation of Star Clusters](#)
- [Formation of Dwarf Galaxies](#)
- [Enrichment of the Intergalactic Medium](#)

● [THEORETICAL MODELS](#)

● [SUMMARY](#)

● [REFERENCES](#)

Next

[Next](#)[Contents](#)

1. INTRODUCTION

One of the most important discoveries from extragalactic observations at mid- and far-infrared wavelengths has been the identification of a class of "infrared galaxies", objects that emit more energy in the infrared ($\sim 5\text{-}500\mu\text{m}$) than at all other wavelengths combined. The first all-sky survey at far-infrared wavelengths carried out in 1983 by the *Infrared Astronomical Satellite (IRAS)* resulted in the detection of tens of thousands of galaxies, the vast majority of which were too faint to have been included in previous optical catalogs. It is now clear that part of the reason for the large number of detections is the fact that the majority of the most luminous galaxies in the Universe emit the bulk of their energy in the far-infrared. Previous assumptions, based primarily on optical observations, about the relative distributions of different types of luminous galaxies - e.g. starbursts, Seyferts, and quasi-stellar objects (QSOs) - need to be revised.

The bulk of the luminosity produced in galaxies bolometrically more luminous than $\sim 4 L^*$ (i.e. $L_{\text{bol}} \gtrsim 10^{11} L_{\odot}$) appears to be produced in objects that are heavily obscured by dust. Although luminous infrared galaxies (hereafter LIGs: $L_{\text{IR}} > 10^{11} L_{\odot}$) are relatively rare objects, reasonable assumptions about the lifetime of the infrared phase suggest that a substantial fraction of all galaxies with $L_{\text{B}} > 10^{10} L_{\odot}$ pass through such a stage of intense infrared emission ([Soifer et al. 1987b](#)).

Substantial progress has been made in cataloging infrared galaxies detected in the *IRAS* database, allowing for a good determination of the luminosity function over a wide range of infrared luminosity ($L_{\text{IR}} \sim 10^7\text{-}10^{13} L_{\odot}$). A brief review of *IRAS* galaxy redshift surveys and a comparison of the infrared galaxy luminosity function with other classes of extragalactic objects is given in [Section 3](#). [Section 4](#) reviews published multiwavelength data for complete samples of the brightest infrared sources and selected samples of the most luminous infrared objects. [Section 5](#) discusses the origin and evolution of LIGs and presents detailed data for several well-studied objects. Several important phenomena associated with LIGs that may significantly impact other areas of extragalactic research are reviewed in [Section 6](#), and [Section 7](#) briefly discusses how theoretical simulations are being used to more accurately interpret the observed morphology and kinematics of both the gas and dust in LIGs.

This review is the first to focus almost exclusively on the properties of luminous infrared galaxies. Pre-*IRAS* reviews of extragalactic infrared observations by [Neugebauer et al. \(1971\)](#) and [Rieke & Lebofsky \(1979\)](#) include discussions of luminous infrared emission from optically selected objects. [Soifer et al.](#)

[\(1987a\)](#) present a broad overview of the extragalactic sky as seen by *IRAS*, including a detailed discussion of the infrared galaxy luminosity function and some discussion of the properties of a few selected LIGs, while the review by [Telesco \(1988\)](#) provides an excellent complimentary summary focusing on the properties of nearby, lower luminosity infrared galaxies. Recent reviews by [Young & Scoville \(1991\)](#) on the molecular gas properties of galaxies and by [Barnes & Hernquist \(1992\)](#) on theoretical models of interacting galaxies cover topics that are particularly relevant to the study of LIGs.

[Next](#)

[Contents](#)

[Next](#)[Contents](#)[Previous](#)

2. BACKGROUND

2.1 Pre-IRAS

The fact that some galaxies emit as much energy in the infrared as at optical wavelengths was established with the first mid-infrared observations of extragalactic sources ([Low & Kleinmann 1968](#); [Kleinmann & Low 1970a, b](#)). Observations of both optical- and radio-selected objects at wavelengths of 2-25 μm uncovered several objects - including luminous starbursts, Seyferts, and QSOs - with "similar infrared continua" that appeared to emit most of their luminosity in the far-infrared. More accurate photometry of a larger number of sources ([Rieke & Low 1972](#)) provided further evidence for dominant infrared emission from Seyfert galaxies and the nuclei of relatively normal spiral galaxies and also singled out several "ultrahigh" infrared luminous galaxies whose extrapolated luminosity at far-infrared wavelengths rivaled the bolometric luminosity of QSOs. A tight correlation between the 21-cm radio continuum and 10- μm infrared fluxes was established for "Seyfert and related galaxies", although the relevance of this correlation for determining the nature of the dominant energy source in these objects was not discussed.

The first critical evidence that the infrared emission from Seyferts was not direct synchrotron radiation was provided by monitoring of the 10- μm flux from the archetypal Seyfert 2 galaxy [NGC 1068](#), which failed to show evidence for variability ([Stein et al. 1974](#)), plus measurements that showed the infrared source to be extended at 10 μm ([Becklin et al. 1973](#)). The infrared spectrum appeared to be better explained by models of thermal reradiation from dust (e.g. [Rees et al. 1969](#), [Burbidge & Stein 1970](#)). More extensive mid-infrared photometry of larger samples of Markarian Seyferts and starbursts ([Rieke & Low 1975](#), [Neugebauer et al. 1976](#)), Seyfert galaxies ([Rieke 1978](#)), and bright spirals ([Rieke & Lebofsky 1978](#), [Lebofsky & Rieke 1979](#)), plus far-infrared (30-300 μm) observations of nearby bright galaxies ([Harper & Low 1973](#), [Telesco & Harper 1980](#)) showed that "infrared excess" was indeed a common property of extragalactic objects, and that the shape of the infrared continuum in most of these sources, with the possible exception of Seyfert 1 galaxies and QSOs, could best be understood in terms of thermal emission from dust. Although star formation seemed to be the most obvious explanation for the dominant energy source in normal galaxies and starbursts, a dust-enshrouded active galactic nucleus (AGN) remained a plausible model for Seyferts and QSOs.

A class of objects that would prove to be particularly relevant to LIGs were those objects in catalogs of interacting and peculiar galaxies (e.g. [Vorontsov-Velyaminov 1959](#), [Arp 1966](#), [Zwicky & Zwicky 1971](#)).

The classic papers by [Toomre & Toomre \(1972\)](#), and [Larson & Tinsley \(1978\)](#) called attention to the role of interactions in triggering extreme nuclear activity, as well as more widespread starbursts¹. [Condon & Dressel \(1978\)](#) and [Hummel \(1980\)](#) found that the 21-cm radio continuum in the nuclei of interacting galaxies was enhanced (by factors of 2-3) compared to isolated spirals. [Condon et al. \(1982\)](#) later interpreted the radio continuum morphology of a class of "bright radio spiral galaxies" as evidence for powerful nuclear starbursts, the majority of which seemed to be triggered by galaxy interactions. [Heckman \(1983\)](#), following a suggestion by [Fosbury & Wall \(1979\)](#) that systems identified as "ongoing mergers" by [Toomre \(1977\)](#) might be exceptionally radio-loud, found that these and similar systems identified from the *Arp atlas* ([Arp 1966](#)) were ~ 8 times more likely to be radio-loud than single spirals with the same total optical luminosity, although it was not clear whether this enhanced radio activity was due to an AGN or a starburst.

Extremely strong mid-infrared and radio continuum emission in the interacting galaxy system Arp 299 (NGC 3690/IC 694) ([Ghez et al. 1983](#)) was interpreted as evidence for "super starbursts" involving several regions, each forming $\gtrsim 10^9 M_{\odot}$ of stars in bursts and lasting $\sim 10^8$ years (although the most luminous infrared source, associated with the nucleus of IC 694, appeared to be powered by an AGN). Surveys of interacting galaxies in the mid-infrared ([Joseph et al. 1984a](#), [Lonsdale et al. 1984](#), [Cutri & McAlary 1985](#)) revealed an enhancement of infrared emission in interacting systems (typically by factors of 2-3) compared to isolated galaxies. [Joseph & Wright \(1985\)](#) identified a subset of advanced mergers in the *Arp atlas* with extremely strong mid-infrared emission that they described as "ultraluminous" infrared galaxies; they argued that super starbursts may occur in the evolution of most mergers.

2.2 Early IRAS Results

IRAS was the first telescope with sufficient sensitivity to detect large numbers of extragalactic sources at mid- and far-infrared wavelengths ([Neugebauer et al. 1984](#)). *IRAS* surveyed ~ 96% of the sky, producing an initial *IRAS Point Source Catalog* (1988; hereafter PSC) with a completeness limit of ~ 0.5 Jy at 12 μm , 25 μm , and 60 μm , and ~ 1.5 Jy at 100 μm . It contained ~ 20,000 galaxies, the majority of which had not been previously cataloged. [Table 1](#) lists the definitions that have generally been adopted as standards for computing the broad-band infrared properties of *IRAS* galaxies.

Table 1. Abbreviations and definitions^a

F_{fir}	$1.26 \times 10^{-14} \{2.58 f_{60} + f_{100}\} [\text{W m}^{-2}]$
L_{fir}	$L(40\text{-}500 \mu\text{m}) = 4\pi D_L^2 C F_{\text{fir}} [L_{\odot}]$
F_{ir}	$1.8 \times 10^{-14} \{13.48 f_{12} + 5.16 f_{25} + 2.58 f_{60} + f_{100}\} [\text{W m}^{-2}]$
L_{ir}	$L(8\text{-}1000 \mu\text{m}) = 4\pi D_L^2 F_{\text{ir}} [L_{\odot}]$
$L_{\text{ir}}/L_{\text{B}}$	$F_{\text{ir}} / \int f_{\nu} (0.44 \mu\text{m})$

LIG Luminous Infrared Galaxy, $L_{\text{ir}} > 10^{11} L_{\odot}$

ULIG UltraLuminous Infrared Galaxy, $L_{\text{ir}} > 10^{12} L_{\odot}$

HyLIG HyperLuminous Infrared Galaxy, $L_{\text{ir}} > 10^{13} L_{\odot}$

^a Throughout this review we adopt $H_0 = 75 \text{ km s}^{-1} \text{ Mpc}^{-1}$, $q_0 = 0$. A luminosity quoted at a specific wavelength refers to $\nu L_{\nu}(\lambda)$, and is given in units of solar bolometric luminosity ($3.83 \times 10^{33} \text{ ergs s}^{-1}$). The quantities $f_{12}, f_{25}, f_{60}, f_{100}$ are the *IRAS* flux densities in Jy at 12, 25, 60, and $100 \mu\text{m}$. The broad-band far-infrared luminosity, L_{fir} , is computed using the prescription given in Appendix B of *Cataloged Galaxies and Quasars Observed in the IRAS Survey* (1985). The scale factor C (typically in the range 1.4-1.8) is the correction factor required to account principally for the extrapolated flux longward of the *IRAS* $100 \mu\text{m}$ filter. D_L is the luminosity distance. L_{fir} has mostly been replaced by the quantity L_{ir} , which better represents the total mid- and far-infrared luminosity. L_{ir} is computed by fitting a single temperature dust emissivity model ($\epsilon \propto \nu^{-1}$) to the flux in all four *IRAS* bands and should be accurate to $\pm 5\%$ for dust temperatures in the range 25-65K (Perault 1987).

Although some previously cataloged objects would prove to have extreme infrared properties, the vast majority were more modest infrared emitters as typified by the results reported by [de Jong et al. \(1984\)](#) for galaxies in the Shapley-Ames catalog. In a sample of 165 SA galaxies, *IRAS* detected nearly all late-type spirals (Sb-Sd) and Irr-Am galaxies, approximately half of the early type, S0-Sa, galaxies and *none* of the ellipticals. For those galaxies detected, $L_{\text{ir}}/L_B = 0.1-5$, with a mean value of ~ 0.4 . The few objects with $L_{\text{ir}}/L_B > 2$ were typically SBs or irregulars. Objects with higher L_{ir}/L_B ratios tended to have warmer f_{60}/f_{100} colors. The classic starburst galaxies [M82](#) and [NGC 253](#) had L_{ir}/L_B ratios of 3 and 5, and $L_{\text{ir}} = 10^{10.3}$ and $10^{10.8} L_{\odot}$ respectively. No objects were found with $L_{\text{ir}} > 10^{11} L_{\odot}$.

The more extreme infrared properties of infrared-selected samples are typified by objects in the *IRAS* minisurvey ([Rowan-Robinson et al. 1984](#)). For a complete flux-limited sample of 86 infrared-selected galaxies from the minisurvey, [Soifer et al. \(1984a\)](#) found that virtually all had $L_{\text{ir}} > 10^{10} L_{\odot}$ and ratios $L_{\text{ir}}/L_B = 1-50$, with the fraction of interacting galaxies being as high as one fourth. More intriguing were the 9 "unidentified" sources ($L_{\text{ir}}/L_B > 50$) which had no obvious optical counterparts in galaxy catalogs and often no visible counterpart on the Palomar Sky Survey plates ([Houck et al. 1984](#)). Initial cross-correlation of larger *IRAS* source lists with galaxy catalogs had produced only one or two objects with similar extreme ratios, most notably the ULIG [Arp 220](#) ([Soifer et al. 1984b](#)) and [NGC 6240](#) ([Wright et al. 1984](#), [Joseph et al. 1984b](#)). Ground-based observations of the unidentified minisurvey objects quickly led to the discovery of faint galaxies, typically at redshifts 0.1-0.2 ([Aaronson & Olszewski 1984](#), [Houck](#)

et al. 1985, [Antonucci & Olszewski 1985](#), [Allen et al. 1985](#), [Iyengar & Verma 1984](#)), implying that these objects also had "ultra-high" infrared luminosities, typically $L_{\text{ir}} \gtrsim 10^{12} L_{\odot}$, and $L_{\text{ir}} / L_{\text{B}} = 30\text{-}400$. None of these objects showed obvious evidence for an active nucleus.

IRAS surveys of optically selected Seyfert galaxies ([Miley et al. 1985](#)) and QSOs ([Neugebauer et al. 1985](#) [1986](#)) showed that active galaxies could be strong far-infrared emitters; most optically selected AGNs had ratios $L_{\text{ir}} / L_{\text{B}}$ in the range 0.2 to 1.0 with higher values in only a small number of objects. However, the full range of infrared excess exhibited by active galaxies is indeed much larger (e.g. [Fairclough 1986](#)). [de Grijp et al. \(1985\)](#) found that searches based on "warm" ($f_{25} / f_{60} \gtrsim 0.3$) colors could be useful for discovering new infrared-luminous active galaxies in the *IRAS* database. This technique appeared to have been motivated by the shape of the infrared spectrum of the Seyfert2 galaxy [NGC 1068](#) ([Telesco & Harper 1980](#)) and the discovery of a similar "warm" 25- μm component in the broad-line, infrared-luminous radio galaxy [3C 390.3](#) ([Miley et al. 1984](#)). Early statistics suggested that the true space density of AGNs could be a factor of two larger than previously assumed with the majority of the new infrared selected objects being a mixture of LINERS and Seyfert2s.

¹ We adopt here the definition of a starburst given by [Larson & Tinsley \(1978\)](#) as a "burst" in the star formation rate of duration $\sim 10^7\text{-}10^8$ years, involving up to 5% of the total stellar mass. [Back](#).

[Next](#)[Contents](#)[Previous](#)


[Next](#)
[Contents](#)
[Previous](#)

3. REDSHIFT SURVEYS

A more complete description of the properties of infrared galaxies became possible only after the determination of redshifts for relatively large unbiased samples of infrared selected objects. [Table 2](#) lists the major published redshift catalogs for *IRAS* galaxies [[Saunders et al. \(1990\)](#) provides a good reference for *IRAS* galaxy surveys prior to 1990].

Table 2. *IRAS* galaxy redshift surveys

Name	Flux limit(s)	Area	Sources ^a	Reference ^b
		<u>all sky</u> ^c		
RBGS	$f_{60} \geq 5.24$ Jy	$ b > 5^\circ$	602 P	Sanders et al. 1996a
1.2 Jy Survey	$f_{60} \geq 1.2$ Jy	$ b > 10^\circ$	5321 P	Fisher et al. 1995
1 Jy ULIGs	$f_{60} \geq 1.0$ Jy	$ b > 30^\circ$	115 F	Kim & Sanders 1996
QDOT	$f_{60} \geq 0.59$ Jy	$ b > 10^\circ$	2387 F	Lawrence et al. 1996
12 μ m Survey	$f_{12} \geq 0.22$ Jy	$ b > 25^\circ$	893 F	Rush et al. 1993
		<u>small area</u>		
2 Jy Survey &	$f_{60} \geq 2.0$ Jy	1072 deg ²	70 P	Smith et al. 1987
Bootes Void	$f_{60} \geq 0.75$ Jy	1423 deg ²	379 P	Strauss & Huchra 1988
KOS-KOSS	$f_{60} \geq 0.6$ Jy	142 deg ²	63 P	Vader & Simon 1987b
NGW	$f_{60} \geq 0.5$ Jy	844 deg ²	389 P	Lawrence et al. 1986
FSS-z	$f_{60} \geq 0.2$ Jy	1310 deg ²	~ 3600 F	Oliver et al. 1996
Pointed Obs	$f_{60} \geq 0.15$ Jy	18 deg ²	66 A	Lonsdale & Hacking 1989
NEPR	$f_{60} \geq 0.05$ Jy	6 deg ²	76 D	Ashby et al. 1996

		<u>color selected</u>		
AGN Candidates	$1 > f_{25} / f_{60} > 0.27$	$ b > 20^\circ$	563 P	de Grijp et al. 1992
WEO	$3 > f_{25} / f_{60} > 0.25$	$ b > 30^\circ$	187 P	Low et al. 1988
Tepid FIRGs	$f_{25} / f_{60} < 0.27$ $f_{60} / f_{100} > 0.78$		53 P	Armus et al. 1989
60 μ m Peakers	$1 > f_{25} / f_{60} > 0.25$ $f_{60} / f_{100} > 1$	$ b > 10^\circ$	51 P	Vader et al. 1993

^a *IRAS* Catalogs: (P) PSC (1988), (F) FSC ([Moshir et al. 1992](#)), (A) Pointed Observations ([Young et al. 1986](#)), (D)

Deep Survey ([Hacking & Houck 1987](#)).

^b References for earlier versions of surveys:

RBGS - [Soifer et al. 1986](#), [1987b](#), [1989](#) (BGS); [Sanders et al. 1995](#) (BGS-Part II),

1.2 Jy Survey - [Strauss et al. 1992](#) (1.936 Jy Survey),

QDOT - [Lawrence et al. 1989](#) (QCD),

12 μ m Survey - [Spinoglio & Malkan 1989](#),

Tepid FIRGs - [Heckman et al. 1987](#).

^c 1 Jy ULIGs - $|b| > 30^\circ$ and $\delta \geq -40^\circ$,

QDOT-1 in 6 random source selection.

3.1 Luminosity Functions

A comparison of the luminosity function of infrared bright galaxies with other classes of extragalactic objects is shown in [Figure 1](#). At luminosities below $10^{11} L_\odot$, *IRAS* observations confirm that the majority of optically selected objects are relatively weak far-infrared emitters ([Bothun et al. 1989](#), [Knapp et al. 1989](#), [Devereux & Young 1991](#), [Isobe & Feigelson 1992](#)). Surveys of Markarian galaxies ([Deutsch & Willner 1986](#), [Mazzarella & Balzano 1986](#), [Mazzarella et al. 1991](#), [Bicay et al. 1995](#)) confirm that both Markarian starbursts and Seyferts have properties (e.g. f_{60}/f_{100} and $L_{\text{ir}} / L_{\text{B}}$ ratios) closer to infrared selected samples as does the subclass of optically selected interacting galaxies (e.g. [Bushouse 1987](#), [Kennicutt et al. 1987](#), [Bushouse et al. 1988](#), [Sulentic 1989](#)); however relatively few objects in optically selected samples are found with $L_{\text{ir}} > 10^{11.5} L_\odot$.

The high luminosity tail of the infrared galaxy luminosity function is clearly in excess of what is

expected from the Schechter function. A better description (e.g. [Soifer et al. 1987b](#)) is a double power law with slope ≈ -1 at low luminosity, changing to a slope of ~ -2.35 at $L_{\text{bol}} \gtrsim 10^{10.3} L_{\odot}$. For $L_{\text{bol}} = 10^{11}$ - $10^{12} L_{\odot}$, LIGs are as numerous as Markarian Seyferts and ~ 3 times more numerous than Markarian starbursts. Ultraluminous infrared galaxies (hereafter ULIGs: $L_{\text{IR}} > 10^{12} L_{\odot}$) appear to be ~ 2 times more numerous than optically selected QSOs, the only other previously known population of objects with comparable bolometric luminosities.

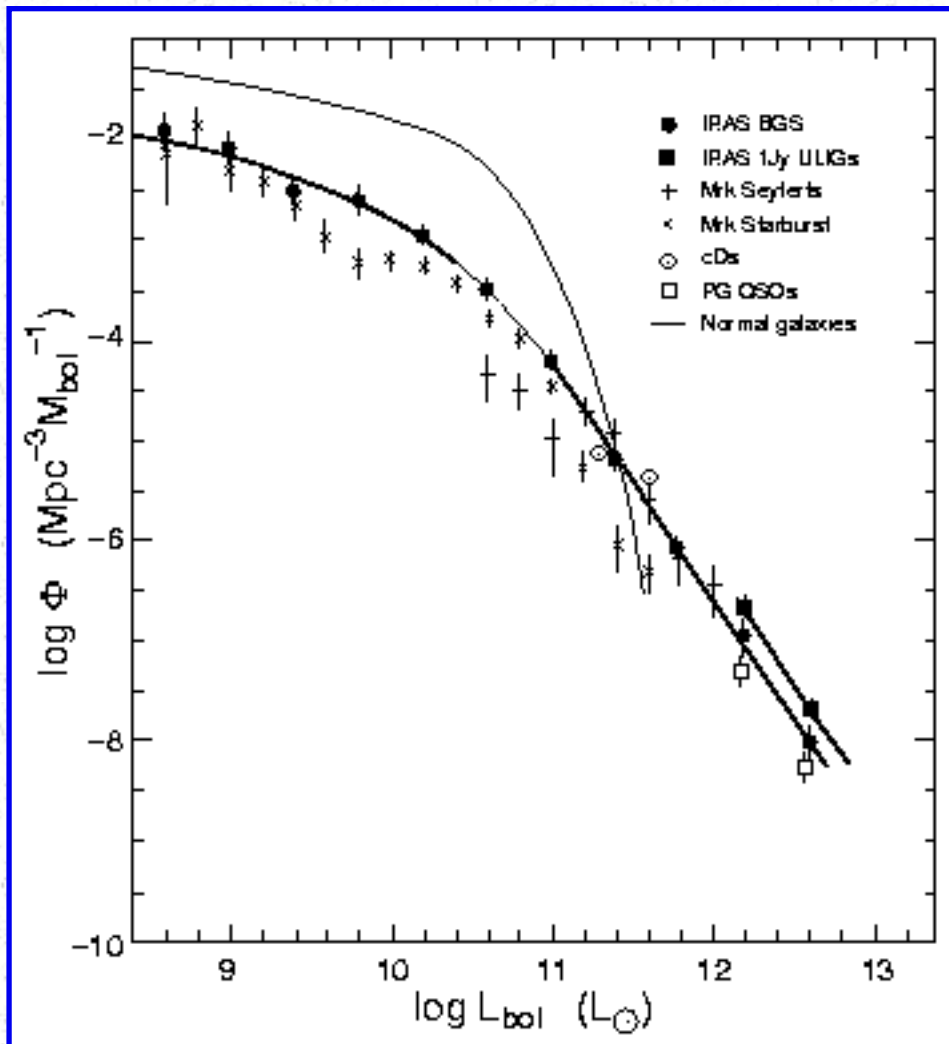


Figure 1. The luminosity function for infrared galaxies compared with other extragalactic objects. References: *IRAS* RBGS ([Sanders et al. 1996a](#)), *IRAS* 1-Jy Survey of ULIGs ([Kim 1995](#)), Palomar-Green QSOs ([Schmidt & Green 1983](#)), Markarian starbursts and Seyfert galaxies ([Huchra 1977](#)), and normal galaxies ([Schechter 1976](#)). Determination of the bolometric luminosity for the optically selected samples was as described in [Soifer et al. \(1986\)](#), except for the adoption of a more accurate bolometric correction for QSOs of $11.8 \times \nu L_{\nu}(0.43 \mu\text{m})$ ([Elvis et al. 1994](#)).

Although LIGs comprise the dominant population of extragalactic objects at $L_{\text{bol}} > 10^{11} L_{\odot}$, they are still relatively rare. For example, [Figure 1](#) suggests that only one object with $L_{\text{ir}} > 10^{12} L_{\odot}$ will be found out to a redshift of ~ 0.033 , and indeed, [Arp 220](#) ($z = 0.018$) is the only ULIG within this volume. The total infrared luminosity from LIGs in the *IRAS* Bright Galaxy Survey (BGS) is only $\sim 6\%$ of the infrared emission in the local Universe ([Soifer & Neugebauer 1991](#)).

Comparison of the space density of ULIGs in the 1-Jy Survey with "local" ULIGs from the BGS provides some evidence for possible strong evolution in the luminosity function at the highest infrared luminosities. Assuming pure density evolution of the form $\phi(z) \propto (1+z)^n$, [Kim \(1995\)](#) found $n \sim 7 \pm 3$ for the complete 1-Jy sample of ULIGs, the uncertainty being influenced primarily by the small range of redshift ($z_{\text{max}} = 0.27$) and the apparent effects of local large scale structure: Nearly all of the evidence for strong evolution comes from ULIGs at flux levels $f_{60} = 1\text{-}2$ Jy corresponding to sources at $z \gtrsim 0.13$. No evidence for evolution is found for the subsample of 2 Jy ULIGs, i.e. $n = 3.8 \pm 3$ ([Kim & Sanders 1996](#)). These results appear to be consistent with previous debates in the literature which find $n \sim 5\text{-}7$ for redshift surveys with flux limits $f_{60} \sim 0.5$ Jy ([Saunders et al. 1990](#), [Oliver et al. 1995](#)) but only $n \sim 3\text{-}4$ for surveys with flux limits $f_{60} \gtrsim 1.5$ Jy ([Fisher et al. 1992](#)), and with analyses of *IRAS* extragalactic source counts ([Hacking et al. 1987](#), [Lonsdale & Hacking 1989](#), [Lonsdale et al. 1990](#), [Gregorich et al. 1995](#)) that show evidence for strong evolution only at relatively low flux levels ($f_{60} \lesssim 1$ Jy). More definitive tests of whether the luminosity function for ULIGs indeed evolves strongly, and how this may compare, for example, with the strong evolution seen for the most luminous QSOs (e.g. [Schmidt & Green 1983](#)), will need to wait for future more sensitive infrared surveys.

3.2 Spectral Energy Distributions

The infrared properties for the complete *IRAS* BGS have been summarized and combined with optical data to determine the relative luminosity output from galaxies in the local Universe at wavelengths $\sim 0.1\text{-}1000 \mu\text{m}$ ([Soifer & Neugebauer 1991](#)). [Figure 2](#) uses data from [Sanders et al. \(1996a, b\)](#) and [Kim \(1995\)](#) to illustrate how the shape of the mean spectral energy distribution (SED) varies for galaxies with increasing total infrared luminosity. Systematic variations are observed in the mean infrared colors; the ratio f_{60}/f_{100} increases while f_{12}/f_{25} decreases with increasing infrared luminosity. [Figure 2](#) also illustrates that the observed range of over 3 orders of magnitude in L_{ir} for infrared-selected galaxies is accompanied by less than a factor of 3-4 change in the optical luminosity.

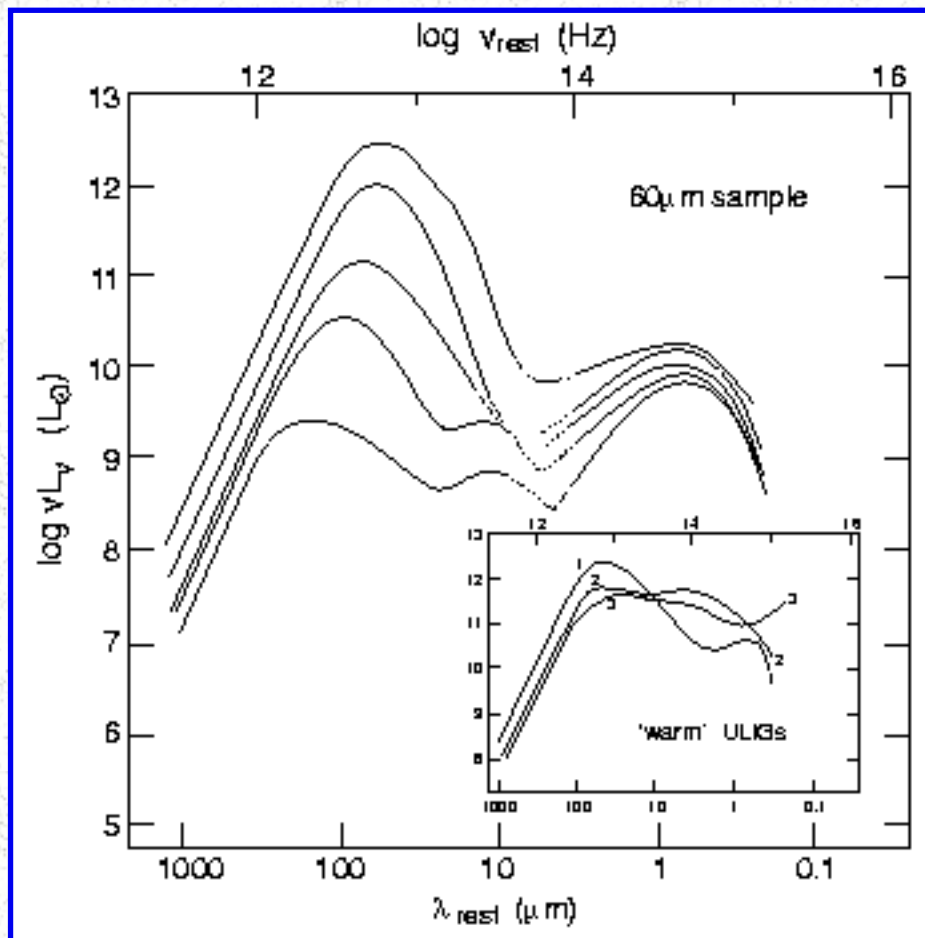


Figure 2. Variation of the mean SEDs (from submillimeter to UV wavelengths) with increasing L_{ir} for a $60 \mu\text{m}$ sample of infrared galaxies. (*Insert*) Examples of the subset ($\sim 15\%$) of ULIGs with “warm” infrared color ($f_{25} / f_{60} > 0.3$). Data for the three objects (1 - the powerful Wolf-Rayet galaxy [IRAS 01003-2238](#), 2 - the “infrared QSO” [IRAS 07598+6508](#), 3 - the optically selected QSO [I Zw 1](#)) are from [Sanders et al. \(1988b\)](#).

Various models of the infrared emission (e.g. [Helou 1986](#), [Rowan-Robinson 1986](#), [Rowan-Robinson & Efsthathiou 1993](#)) have suggested that in lower luminosity “normal” galaxies the secondary peak in the mid-infrared is due to emission from small dust grains near hot stars, while the stronger peak at $\lambda \gtrsim 100$ - $200 \mu\text{m}$ represents emission dominated by dust from infrared cirrus ($T_{\text{D}} \lesssim 20 \text{ K}$) heated substantially by the older stellar population. In more infrared luminous galaxies a “starburst” component emerges ($T_{\text{D}} \sim 30$ - 60 K) with a peak closer to $60 \mu\text{m}$, plus, in Seyfert galaxies, an even warmer component ($T_{\text{D}} \sim 150$ - 250 K) peaking near $25 \mu\text{m}$, presumably representing warm dust directly heated by the AGN.

[Sanders et al. \(1988b\)](#) showed that a small but significant fraction of ULIGs, those with “warm” ($f_{25} / f_{60} > 0.3$) infrared colors, have SEDs with mid-infrared emission (~ 5 - $40 \mu\text{m}$) over an order of magnitude stronger than the larger fraction of “cooler” ULIGs. These warm galaxies ([Figure 2](#) insert), which appear

to span a wide range of classes of extragalactic objects including powerful radio galaxies (PRGs: $L_{408\text{MHz}} \gtrsim 10^{25} \text{ W Hz}^{-1}$) and optically selected QSOs, have been used as evidence for an evolutionary connection between ULIGs and QSOs (e.g. [Sanders et al. 1988a, b](#)). This connection is strengthened by *IRAS* data for QSOs ([Figure 3](#)), which shows that the mean SED of optically selected QSOs is dominated by thermal emission from an infrared/submillimeter bump ($\sim 1\text{-}300 \mu\text{m}$) in addition to the "big blue bump" ($\sim 0.05\text{-}1 \mu\text{m}$); the former is typically 30% as strong as the latter and is presumably thermal emission from dust in an extended circumnuclear disk surrounding the active nucleus.

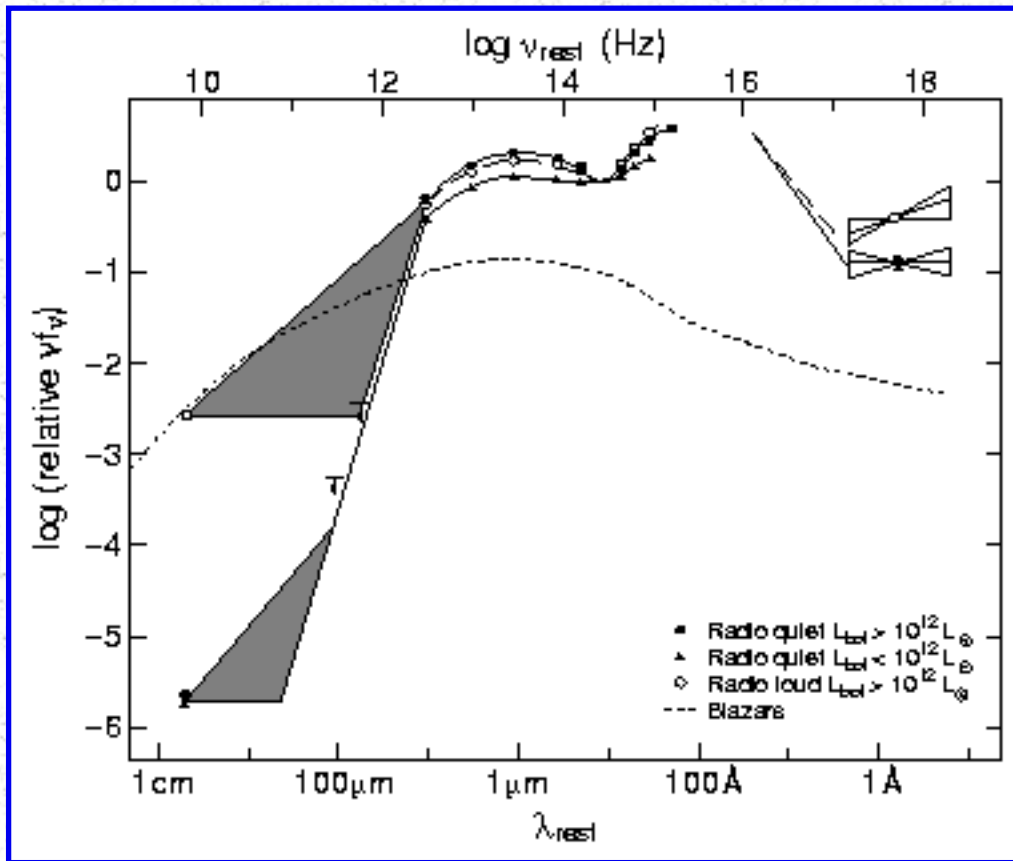


Figure 3. Mean spectral energy distributions from radio to X-ray wavelengths of optically selected radio-loud and radio-quiet QSOs ([Sanders et al. 1989a](#)), and Blazars ([Impey & Neugebauer 1988](#)).

[Next](#)
[Contents](#)
[Previous](#)


[Next](#)
[Contents](#)
[Previous](#)

4. PROPERTIES OF LUMINOUS INFRARED GALAXIES

Substantial multiwavelength observations now exist for large samples of *IRAS* galaxies; the most extensive and highest spatial resolution observations are of objects in the BGS. Data for LIGs are summarized below by wavelength region. Wherever possible, emphasis is placed on trying to understand the variation of the properties of LIGs as a function of infrared luminosity.

4.1 Optical and Near-Infrared Imaging

Early optical imaging studies of *IRAS* galaxies are largely split into two groups: morphological classifications of relatively bright infrared sources that had previously been cataloged in optical surveys and observations of the most luminous infrared sources or sources selected for their extreme infrared properties (typically high infrared-to-blue or extreme color temperature). The former captured, almost exclusively, relatively nearby objects with $L_{\text{ir}} < 10^{11} L_{\odot}$ and can be summarized by the results from [Rieke & Lebofsky \(1986\)](#), who found that nearly all E's and most S0s have $L_{\text{ir}} < 10^9 L_{\odot}$, with most spirals having higher infrared luminosities; for $L_{\text{ir}} = 10^{10}$ - $10^{11} L_{\odot}$, nearly all of the sources were Sb or Sc galaxies. It also appeared that ~ 12-25% of LIGs were peculiar or interacting systems (e.g. [Soifer et al. 1984a](#)). A much higher proportion of interacting and disturbed systems was reported from samples selected on the basis of extreme infrared properties. The most luminous sources ($L_{\text{ir}} \gtrsim 3 \times 10^{12} L_{\odot}$) in the *IRAS* database ([Kleinmann & Keel 1987](#); [Sanders et al. 1987b, 1988b](#); [Hutchings & Neff 1987](#); [Vader & Simon 1987a](#)) were universally classified as strong interactions/mergers. Sources with high $L_{\text{ir}} / L_{\text{B}}$ ratios (e.g. [van den Broek 1990](#); [Klaas & Elsässer 1991, 1993](#)), or warm colors, either f_{60} / f_{100} or f_{25} / f_{60} colors (e.g. [Armus et al. 1987, 1990](#); [Sanders et al. 1988b](#); [Heisler & Vader 1994](#)), were predominantly ($\gtrsim 70\%$) strongly interacting/peculiar systems, with the remaining objects often being amorphous or elliptical-like in appearance.

More recent data for the complete BGS now shows that the fraction of objects in that are interacting/merger systems appears to increase systematically with increasing infrared luminosity. Images of objects in the BGS ([Sanders et al. 1988a, 1996a](#); [Melnick & Mirabel 1990](#)) show that the fraction of strongly interacting/merger systems increases from ~ 10% at $L_{\text{ir}} / L_{\odot} = 10.5$ -11 to ~ 100% at $L_{\text{ir}} / L_{\odot} > 12$. [Figure 4](#) shows images of the complete sample of 10 ULIGs in the original BGS ([Sanders et al. 1988a](#)). Other studies of ULIGs have generally reached a similar conclusion that $\gtrsim 95\%$ are merger systems ([Kim](#)

1995, [Murphy et al. 1996](#), [Clements et al. 1996](#); although see [Lawrence et al. 1989](#), [Leech et al. 1994](#)).

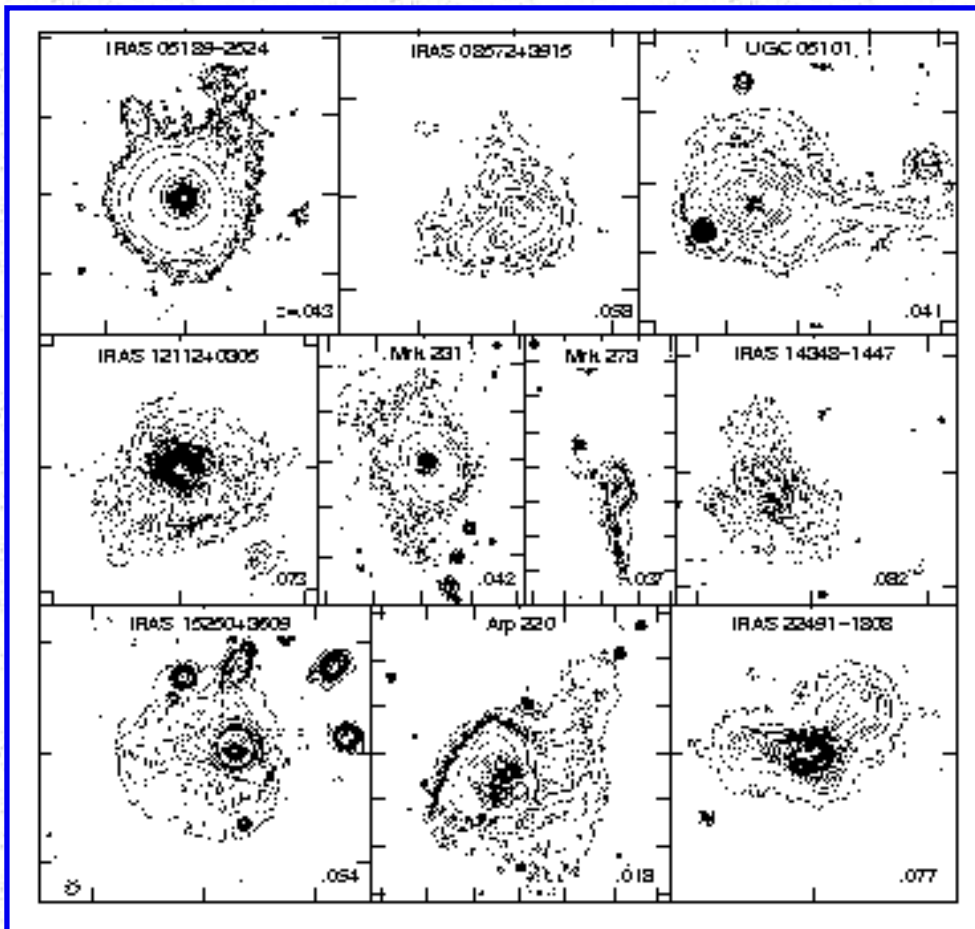


Figure 4. Optical (*r*-band) CCD images of the complete sample of ten ULIGs from the original BGS ([Sanders et al. 1988a](#)). Tick marks are at 20" intervals.

The improved angular resolution and lower optical depth in the near-infrared as compared to the optical has proved to be particularly useful for disentangling nuclear morphology not seen in the optical data (e.g. [Carico et al. 1990](#), [Graham et al. 1990](#), [Eales et al. 1990](#)). The mean and range of projected nuclear separations for ULIGs in the BGS are ~ 2 kpc and < 0.3 to 10 kpc respectively ([Sanders 1992](#)). More recent *K*-band imaging of larger samples of ULIGs ([Murphy et al. 1996](#), [Kim 1995](#)) generally confirms these results, although a few systems appear to have nuclear separations as large as 20-40 kpc.

Despite their extreme infrared luminosities, photometry of ULIGs confirms that most are only moderately luminous in the optical and near-infrared. For the 10 ULIGs in the original BGS the median blue absolute magnitude is $\text{bar } M_B = -20.7$ ([Jensen et al. 1996](#)) [compared to the mean value $\langle M_B \rangle = -20.2$ reported by [Armus et al. \(1990\)](#) for their more distant sample of "Arp 220-like" objects], $\text{bar } M_r \sim -21.6$ ([Murphy et al. 1996](#); corrected by +0.44 mag by J Surace, private communication), and $\text{bar } M_K = -25.2$ ([Jensen et al. 1996](#)). Compared to an L^* galaxy² the median total luminosities for ULIGs are $\sim 2.5 L_B^*$, $\sim 2.7 L_r^*$, and $\sim 2.5 L_K^*$, where the range around the median (excluding Seyfert 1 objects) is -0.9 to +1.6 mag in M_r and -

1.0 to +2.2 mag in M_K' . Most ULIGs contain compact nuclei, with typically one quarter of the total K' -band luminosity originating in the inner 1" radius, except for the few Seyfert 1 galaxies (e.g. [Mrk 231](#)) where the pointlike nuclear source can be as much as a factor of ~ 5 times stronger than the surrounding galaxy. The typical host galaxies of ULIGs, therefore, appear to be $\sim 2L^*$ at K' .

4.2 Optical and Near-Infrared Spectroscopy

Although extensive optical redshift surveys have been carried out to identify *IRAS* galaxies, much of these data either have spectral resolution that is too low or are too limited in wavelength coverage to be of use for anything more than simple redshift determinations. Higher-resolution observations (typically $\delta\lambda = 3\text{-}5$ Å for $\lambda \sim 3800\text{-}8000$ Å) are now available for most of the *IRAS* galaxies in the imaging studies discussed above. [Elston et al. \(1985\)](#) classified the majority of *IRAS* minisurvey objects as "starbursts taking place in dusty galaxies". On the other hand, $\sim 50\%$ of the objects with "warm" colors, f_{25}/f_{60} , from the sample of [de Grijp et al. \(1985\)](#) were classified as Seyferts, with an additional $\sim 20\%$ classified as LINERS ([Osterbrock & De Robertis 1985](#)). Observations of "warm" objects at fainter flux levels in the *IRAS* database produced the first two infrared selected QSOs ([Beichman et al. 1986](#), [Vader & Simon 1987a](#)) plus several of the most intrinsically luminous infrared sources currently known, all of which are classified as Seyfert 2 in direct emission (e.g. [Kleinman & Keel 1987](#), [Hill et al. 1987](#), [Frogel et al. 1989](#), [Cutri et al. 1994](#)), but have been shown to contain hidden broad-line regions in polarized light ([Hines 1991](#), [Hines & Wills 1993](#), [Hines et al. 1995](#)). [Vader et al. \(1993\)](#) also report that $\sim 60\%$ of their "warm" sample of "60 μm Peakers" are Seyferts.

[Heckman et al. \(1987\)](#) and [Armus et al. \(1989, 1990\)](#) have used long-slit spectroscopy (4500-8000 Å) and narrow-band ($H\alpha + [\text{NII}]$) imaging to show that [Arp 220](#)-like "tepid" LIGs appear to contain huge ($\gtrsim 10$ kpc), powerful emission-line nebulae often characterized by spectacular loops and bubbles, which they interpret as a starburst-driven superwind (see also [Section 6.4](#)). The visible spectrum of these objects appears to be dominated by young stars, with $\sim 20\%$ showing evidence for a substantial intermediate-age population (few $\times 10^8$ years) and another $\sim 20\%$ showing strong Wolf-Rayet lines, indicating a very young starburst ($\lesssim 10^7$ years). The total $H\alpha + \text{N}[\text{II}]$ luminosity (corrected for extinction) is typically a factor of ~ 30 larger than that for isolated spiral galaxies ([Kennicutt & Kent 1983](#)). As a class, these objects are similar to LINERs; about half are intermediate between LINERs and low-excitation H II regions. Steep Balmer decrements imply that they are being viewed through substantial amounts of obscuring dust. These data have been used to suggest that the "Arp 220-phase" may be characterized by an ongoing powerful circumnuclear starburst that may be rapidly clearing out the obscuring gas and dust in the inner few kiloparsecs of these objects.

More recently, the fraction of LIGs of different spectral type has been determined from an analysis of long-slit spectroscopy of complete samples of objects using several diagnostic emission-line ratios (e.g. [Veilleux & Osterbrock 1987](#)). [Figure 5](#) shows the results from an analysis of a complete subsample of objects in the BGS ([Kim et al. 1995](#), [Veilleux et al. 1995](#)), supplemented by a larger sample of ULIGs

([Kim et al. 1996](#)). The percentage of Seyfert galaxies increases systematically from $\sim 4\%$ at $L_{\text{IR}} / L_{\odot} = 10-11$, to $\sim 45\%$ at $L_{\text{IR}} / L_{\odot} > 12.3$, whereas the percentage of LINERs remains relatively constant ($\sim 33\%$) at all infrared luminosities $L_{\text{IR}} / L_{\odot} > 10$.

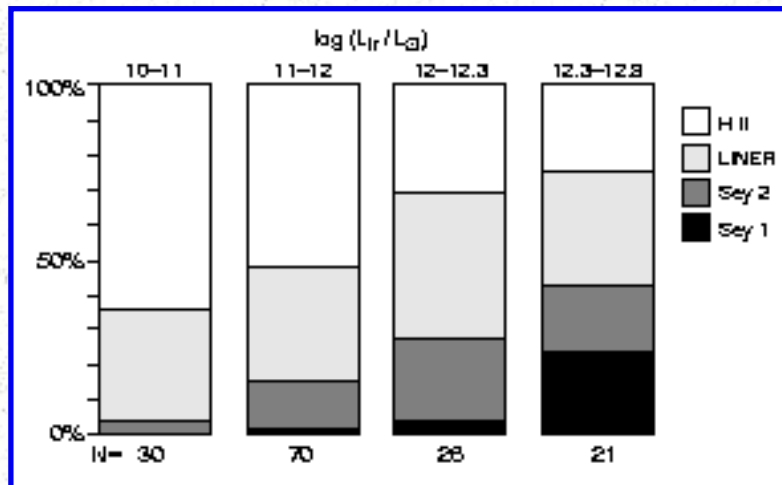


Figure 5. The optical spectral classification of infrared galaxies versus infrared luminosity ([Kim 1995](#)).

The amount of published near-infrared spectroscopy for *IRAS* galaxies is small compared to the available optical data. [Rieke et al. \(1985\)](#) presented a detailed analysis of relatively low-dispersion infrared data at *K* and *L* bands for [NGC 6240](#) and [Arp 220](#), claiming that the former could be powered entirely by a very luminous starburst whereas as much as half of the luminosity in [Arp 220](#) appeared to be due to a Seyfert nucleus. Most of the early low-dispersion data for LIGs have been superseded by spectra covering the *K*-band window at resolving powers $\delta\lambda/\lambda \sim 300-800$ using infrared CCD arrays. [Goldader \(1995\)](#) and [Goldader et al. \(1995\)](#) find that LIGs with Seyfert-like optical classifications also show evidence for dominant non thermal emission in the *K*-band, and most if not all ULIGs with Seyfert 2 optical spectra show evidence for Seyfert 1 linewidths in $\text{Pa}\beta$ ([Goodrich et al. 1994](#)) or $\text{Pa}\alpha$ ([Veilleux et al. 1996](#)); however, for "cool" LIGs, no new broad-line regions are discovered in the near-infrared that were not already seen at optical wavelengths. Perhaps the most intriguing new result is the systematic low value of the $\text{Br}\gamma / \text{H}_2\text{S}(1)$ line ratio in ULIGs as compared with lower luminosity objects, a result that suggests that the dominant luminosity source in ULIGs is still highly obscured even at near-infrared wavelengths ([Goldader et al. 1995](#)). A more detailed analysis of [Arp 220](#) using several infrared lines ([Armus et al. 1995a, b](#)) also suggests that as much as 80-90% of the total luminosity could be powered by an obscured AGN.

For the few hyperluminous infrared galaxies (HyLIGs: $L_{\text{IR}} > 10^{13} L_{\odot}$) that have been discovered in the *IRAS* database, all are at $z \gtrsim 1$, so that near-infrared spectra provide the only means for observing several of the most prominent diagnostic lines (e.g. $\text{H}\alpha$ and $\text{H}\beta$). All of these objects have rest-frame optical emission-line ratios characteristic of Seyferts [e.g. [IRAS 15307+3252](#) ([Soifer et al. 1995](#), [Evans et al. 1996a](#)); [IRAS 10214+4724](#) ([Soifer et al. 1992](#), [1995](#); [Elston et al. 1994](#))].

4.3 Mid- and Far-Infrared (Post-IRAS) Observations

Ground-based observations in the mid-infrared, and far-infrared measurements with the *Kuiper Airborne Observatory (KAO)* have been carried out in an attempt to set meaningful constraints on the size of the infrared emitting region in a few LIGs. [Becklin & Wynn-Williams \(1987\)](#) reported that the 20- μm size of [Arp 220](#) was smaller than 1.5" (500 pc), and they estimated a visual extinction of at least 50 mag based on the depth of a deep silicate absorption feature at 10 μm . [Dudley & Wynn-Williams \(1996\)](#) use the depth of the silicate absorption feature to estimate 10- μm sizes of only a few parsecs for [Arp 220](#) and the warm ULIG [IRAS 08572+3915](#). [Matthews et al. \(1987\)](#) used slit scans to show that the 10- μm source in [Mrk 231](#) was smaller than 1" (800 pc). [Miles et al. \(1996\)](#) have obtained 10- μm maps for 10 LIGs and find that a large fraction ($\sim 65\text{-}100\%$) of the 10- μm emission in ULIGs and warm LIGs originates in an unresolved ($\lesssim 0.6''$) core.

Observations with the *KAO* using drift scans at 50-100 μm ([Joy et al. 1986, 1989](#); [Lester et al. 1987](#)) have shown that the emission regions in a few sources (e.g. [Arp 220](#), [Arp 299](#), [NGC 1068](#)) contain dominant compact ($\lesssim 10''$) components at these wavelengths; however, larger telescopes or interferometers are clearly needed before more meaningful constraints can be set on the size of the far-infrared sources responsible for the bulk of the far-infrared luminosity in LIGs.

4.4 Submillimeter Continuum

Ground-based measurements in the submillimeter continuum ($\sim 350\text{-}860 \mu\text{m}$) have been obtained for a few of the brightest LIGs. [Emerson et al. \(1984\)](#) found that the far-infrared/submillimeter emission from [Arp 220](#) could be fit by a single temperature dust model with $T_{\text{dust}} \sim 60 \text{ K}$, and they derived an optical depth of ~ 1 at 180 μm (!) for an assumed source size of 4". More recently, [Rigopoulou et al. \(1996a\)](#) have interpreted their submillimeter measurements for all ULIGs in the BGS as being consistent with thermal dust emission.

Submillimeter observations of LIGs have also been reported by [Eales et al. \(1989\)](#) and [Clements et al. \(1993\)](#), with the general result that the far infrared/submillimeter continuum in all of the objects can be reasonably fit by a single temperature dust model (assuming a ν^{-2} emissivity law) with dust temperatures of 30-50 K. There is no obvious evidence for large amounts of cooler dust, although large quantities of sufficiently cool dust (i.e. $T_{\text{dust}} \lesssim 20 \text{ K}$) cannot be ruled out (e.g. [Devereux & Young 1991](#)).

4.5 Radio Continuum

A "tight correlation" between the flux in the infrared and the radio continuum has been found in several studies of normal, starburst, and Seyfert galaxies ([van der Kruit 1971](#), [Rieke & Low 1972](#), [Dickey & Salpeter 1984](#), [Helou et al. 1985](#), [Sanders & Mirabel 1985](#), [Wunderlich et al. 1987](#)). [Figure 6a](#) shows that

the logarithmic ratio of far-infrared and radio continuum flux densities, $q = \log \{ [F_{\text{fir}} / (3.75 \times 10^{12} \text{ Hz})] / [f_{\nu} (1.49 \text{ GHz})] \}$, is relatively constant, $q \sim 2.35$, for most LIGs in the BGS, with a rather small dispersion at a given L_{ir} ($\sigma \sim 0.2$). This relationship appears to hold for sources covering several orders of magnitude in L_{ir} , from quiescent disk-like spirals like [M31](#) to the powerful nuclear sources in ULIGs like [Arp 220](#), although there is evidence that the mean changes slightly at both low and high infrared luminosities. At lower infrared luminosities, $\langle q \rangle$ appears to increase slightly as galaxies transit from heating dominated by young stars to heating by an old stellar population ([Condon et al. 1991a](#), [Xu et al. 1994](#)), whereas at the highest infrared luminosities $\langle q \rangle$ increases, apparently due mainly to optical depth effects in the radio ([Condon et al. 1991b](#)). More recently, [Bicay et al. \(1995\)](#) have shown that $\langle q \rangle$ for Markarian starbursts is enhanced by a factor of ~ 3 relative to Markarian Seyferts, but the reason for this increase is not immediately clear.

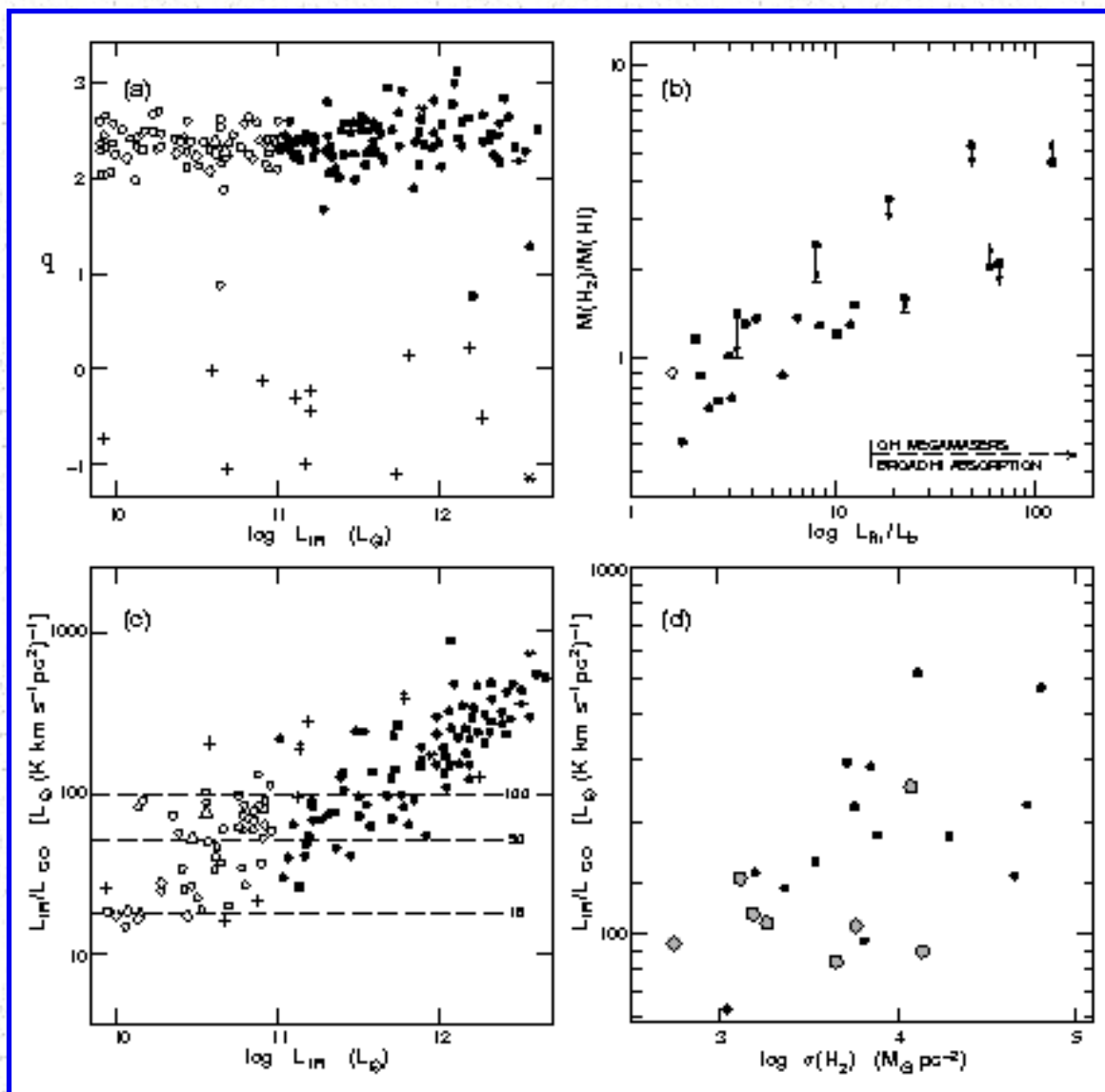


Figure 6. (a) q versus L_{ir} . Solid and open circles represent LIGs and lower luminosity BGS galaxies respectively. Open triangles refer to the nearby starburst galaxies [M82](#) and [NGC 253](#), and open diamonds represent the Milky Way and three "normal" nearby spiral galaxies ([IC 342](#), [NGC 6946](#), [NGC 891](#)). Asterisks refer to optically selected

QSOs that have been detected in CO ([IZw1](#), [Mrk 1014](#), [3C 48](#)), and "+" signs represent PRGs detected by *IRAS*. (b) The ratio of molecular (H_2) to atomic (H I) gas versus the infrared-to-blue luminosity ratio in *IRAS* BGS galaxies ([Mirabel & Sanders 1989](#)). The arrows are due to lower and upper limits in the measurement of the H I fluxes. Most galaxies with $L_{\text{ir}} / L_B \gtrsim 20$ exhibit H I absorption and OH megamaser emission with velocity extents of several hundred km s^{-1} . (c) $L_{\text{ir}} / L'_{\text{CO}}$ versus L_{ir} . The dashed lines represent mean values for nearby "normal" spirals ($L_{\text{ir}}/L'_{\text{CO}} \sim 18$), nearby starburst galaxies ($L_{\text{ir}}/L'_{\text{CO}} \sim 50$), and the most extreme star-forming GMC cores in the Milky Way ($L_{\text{ir}}/L'_{\text{CO}} \sim 100$). (d) Correlation of the central concentration of molecular gas with the $L_{\text{ir}}/L'_{\text{CO}}$ ratio for LIGs in the *IRAS* BGS ([Scoville et al. 1991](#), [Bryant 1996](#)). Small black and larger grey circles represent objects where the spatial resolution was sufficient to resolve circumnuclear regions of < 1 kpc and 1-2 kpc diameter respectively.

Most radio galaxies and radio-loud QSOs have q -values much lower than 2.35 (typically by factors of ~ 2 -4 in the log), usually due to the presence of strong, very-compact radio cores combined with extended radio lobes/jets that are apparently decoupled from the infrared emission. However, evidence exists that radio galaxies still show a correlation in their far-infrared and radio fluxes, but with a value $\langle q \rangle \sim -0.65$ (e.g. [Golombek et al. 1988](#), [Knapp et al. 1990](#), [Impey & Gregorini 1993](#)).

The "radio-infrared correlation" has been used in an attempt to overcome the poor angular resolution of far-infrared instruments. High-resolution radio surveys of LIGs in the BGS were made at 1.49 GHz ([Condon et al. 1990](#)) and at 8.44 GHz ([Condon et al. 1991b](#)). The VLA maps show that nearly all galaxies with $L_{\text{fir}} \lesssim 10^{11} L_{\odot}$ are dominated by extended, diffuse radio emission, whereas most ULIGs are dominated by compact, sub-arcsec radio sources. [Condon et al. \(1991b\)](#) concluded that most LIGs in the BGS - with the exception of the Seyfert 1 galaxy [Mrk 231](#), which is dominated by a variable ultracompact radio source ($\lesssim 1$ pc) - can be modeled by ultraluminous nuclear starbursts (see also [Crawford et al. 1996](#)). These starburst regions would be so dense that they are optically thick even to free-free absorption at $\nu = 1.49$ GHz and to dust absorption at $\lambda \lesssim 25 \mu\text{m}$! If this is true, then X rays, infrared, and radio waves may not be able to probe the dense cores of ULIGs; the far-infrared luminosity is then at best a good calorimeter. Due to Compton scattering in such dense clouds, even a compact source of hard X rays will be hidden from the observer !

As a further probe of the size of the radio sources in LIGs, [Lonsdale et al. \(1993\)](#) carried out a sensitive VLBI survey of 31 objects and found that typically $\sim 12\%$ of the radio flux arises in cores only 5-150 milliarcsec in size (which rules out a single supernova interpretation of the compact radio cores). These compact VLBI cores are comparable in power to the total radio power of typical Seyfert galaxies ([Ulvestad & Wilson 1989](#)) and radio-quiet QSOs ([Kellermann et al. 1989](#)).

4.6 Gas Content

Single-dish observations of millimeter-wave emission from the rotational transitions of CO ($\theta_{\text{FWHM}} \sim 20\text{--}60''$) and the 21-cm line of H I ($\theta_{\text{FWHM}} \sim 3\text{--}10'$) now exist for the majority of objects in the BGS. These data have shown that the total neutral gas content, in particular the total mass of molecular gas, appears to play a critical role in the genesis of LIGs. More recently, interferometer maps of a few dozen LIGs and lower luminosity infrared-selected objects have provided dramatic pictures of the redistribution of the H I and H₂ gas that occurs during interactions and mergers.

4.6.1 ATOMIC GAS (H I) The first observations of LIGs at centimeter wavelengths revealed somewhat perplexing properties. At $\lambda = 21$ cm, the most luminous infrared galaxies showed very broad H I absorption lines, indicating rotation plus large amounts of unusually turbulent neutral gas ([Mirabel 1982](#)). The H I profiles typically show absorption features with widths of a few hundred to up to 1000 km s⁻¹, with total column densities $\gtrsim 10^{21\text{--}22}$ atoms cm⁻². VLA observations of the H I absorption had suggested that most of the absorbing H I is located in the inner few hundred parsecs of these galaxies (e.g. [Baan et al. 1987](#)), in front of the nuclear radio continuum sources. The total masses of H I in a complete sample of galaxies with $L_{\text{fir}} \gtrsim 2 \times 10^{10} L_{\odot}$ are in the range of 5×10^8 to $3 \times 10^{10} M_{\odot}$, with only a weak correlation between $M(\text{H I})$ and L_{fir} ([Mirabel & Sanders 1988](#)).

[Mirabel & Sanders \(1988\)](#) carried out a statistical analysis of the difference between the radial velocities of the H I 21-cm line absorptions and the optical redshifts. Although the discrepancy between the radio and optical velocities is usually smaller than the velocity width of the H I absorptions, there is a clear trend for the radio redshifts to be greater than the optical redshifts. Among 18 galaxies with H I absorption, 15 were found with $V_{\text{H I abs}} > V_{\text{opt}}$ and only 3 with $V_{\text{H I abs}} \leq V_{\text{opt}}$. The mean value of $V_{\text{H I abs}} - V_{\text{opt}}$ is 90 km s⁻¹. From VLA observations [Dickey \(1986\)](#) found a similar trend, from which he estimated an accretion rate of $\sim 1 M_{\odot} \text{ year}^{-1}$ into the nuclear regions.

The optical redshifts may be affected by systematic errors and there are some caveats to the interpretation of the statistical discrepancy between optical and radio velocities as due entirely to infall of H I. The optical redshifts are often determined from emission lines in low dispersion spectra, which due to large scale superwinds (see [Section 6.4](#)) are usually asymmetric with extended blue wings. In this context, some of the statistical discrepancy between the radio and optical redshifts could be due to optical line-emitting gas mixed with dust that is moving radially, probably outward. However, from a careful analysis of the available data, [Martin et al. \(1991\)](#) concluded that most of the H I seen in absorption is indeed infalling toward the central source.

4.6.2 MOLECULAR GAS (H₂) Substantial information on the total molecular gas content of LIGs has been obtained from single-dish observations of millimeter-wave CO emission for large samples of IRAS galaxies. An important discovery has been that *all* LIGs appear to be extremely rich in molecular gas. Early CO observations of infrared selected galaxies (most with $L_{\text{ir}} = 10^{10}\text{--}10^{11} L_{\odot}$) found a rough correlation between CO and far-infrared luminosity ([Young et al. 1984, 1986a, b](#); [Sanders & Mirabel 1985](#)). Assuming a constant conversion factor between CO luminosity and H₂ mass, $M(\text{H}_2) / L'_{\text{CO}} = 4.6$

[$M_{\odot} (\text{K km s}^{-1} \text{ pc}^2)^{-1}$] (e.g. [Scoville & Sanders 1987](#)), total H_2 masses were in the range $\sim 1\text{-}30 \times 10^9 M_{\odot}$, or approximately 0.7 to 20 times the molecular gas content of the Milky Way. [Mirabel & Sanders \(1989\)](#) found that the ratio of total H_2 to H I mass is typically > 1 with some evidence that $M_T(\text{H}_2) / M_T(\text{H I})$ increases with increasing L_{ir} / L_B ([Figure 6b](#)). Multitransition CO measurements (e.g. [Sanders et al. 1990](#), [Radford et al. 1991](#), [Braine et al. 1993](#), [Devereux et al. 1994](#), [Rigopoulou et al. 1996b](#)) and detection of strong emission from dense gas tracers such as HCN ([Solomon et al. 1992a](#)), CS, and HCO^+ (see reviews by [Mauersberger & Henkel 1993](#), [Radford 1994](#), [Gao 1996](#)) indicate that the mean molecular gas temperatures and densities in the central regions of LIGs are hot, $T_{\text{kin}} = 60\text{-}90 \text{ K}$, and dense, $n(\text{H}_2) \sim 10^5\text{-}10^7 \text{ cm}^{-3}$, similar to the conditions in massive Galactic giant molecular cloud (GMC) cores.

Significant improvements in detector performance in the late 1980s resulted in a dramatic increase in the number of extragalactic infrared sources detected in CO. The first objects detected at $z \gtrsim 0.03$ were ULIGs from the BGS; these included the first detection of CO emission from a Seyfert 1 galaxy ([Mrk 231](#): [Sanders et al. 1987b](#)) and two of the most intrinsically luminous CO sources currently known ([VII Zw 31](#): [Sage & Solomon 1987](#); [IRAS 14348-1447](#): [Sanders et al. 1988d](#)). Detections of objects at $z > 0.1$ soon followed, including the first CO detections of UV-excess QSOs ([Mrk 1014](#): [Sanders et al. 1988c](#); [I Zw 1](#): [Barvainis et al. 1989](#)), an infrared selected QSO ([IRAS 07598+6508](#): [Sanders et al. 1989b](#)), a PRG ([4C 12.50](#): [Mirabel et al. 1989](#)), and a radio-loud QSO ([3C 48](#): [Scoville et al. 1993](#)).

[Figure 6c](#) includes data from several single-dish CO(1- \rightarrow 0) surveys of *IRAS* galaxies ([Sanders et al. 1991](#), [Mirabel et al. 1990](#), [Tinney et al. 1990](#), [Downes et al. 1993](#), [Mazzarella et al. 1993](#), [Young et al. 1995](#), [Elfhag et al. 1996](#), [Solomon et al. 1996](#), [Evans 1996](#)) illustrating both the general trend of increasing $L_{\text{ir}}/L'_{\text{CO}}$ ratio with increasing L_{ir} and the fact that this ratio can vary by nearly a factor of 30 at a given L_{ir} . Assuming $M(\text{H}_2) = 4.6 L_{\text{CO}}$, [Figure 6c](#) shows that the *total* molecular gas mass in ULIGs - typically $M(\text{H}_2) \gtrsim 10^{10} M_{\odot}$ - is on average more infrared luminous than any of the most active star-forming Galactic GMC cores [which have diameters typically of $\sim 2\text{-}5 \text{ pc}$ and $M(\text{H}_2) = 10^3\text{-}10^4 M_{\odot}$].

Millimeter-wave interferometer measurements of CO emission have been obtained for approximately two dozen LIGs (e.g. [Scoville et al. 1991](#); [Okumura et al. 1991](#); [Bryant 1996](#); Yun & Hibbard, private communication). [Figure 6d](#) shows that for these objects, nearly all of which are advanced mergers, $\sim 40\text{-}100\%$ of the total CO luminosity, or $M(\text{H}_2) = 1\text{-}3 \times 10^{10} M_{\odot}$ assuming the standard Milky Way conversion factor, is contained within the central $r < 0.5\text{-}1 \text{ kpc}$. The mean surface density in the central 1 kpc regions of ULIGs is typically in the range $\langle \sigma(\text{H}_2) \rangle = 1.5\text{-}7 \times 10^4 M_{\odot} \text{ pc}^{-2}$, although the H_2 masses in these extreme regions may be overestimated by a factor of 2-3 ([Downes et al. 1993](#), [Solomon et al. 1996](#)). Even allowing for such a decrease in the conversion factor, these values are $\sim 50\text{-}250$ times larger than the mean gas surface density in the central 1 kpc of the Milky Way and would seem to imply enormous optical depths ($A_V \sim 200\text{-}1000 \text{ mag}$) along an average line of sight toward the nucleus of these objects. Such high values are consistent with the implied high optical depths in the nuclear regions of

“cool” ULIGs at K -band (see [Section 4.2](#)) and optical depths near unity at $\lambda \sim 200 \mu\text{m}$ implied by the far-infrared/submillimeter measurements for [Arp 220](#) (see [Section 4.4](#)).

4.6.3 OH MEGAMASERS The high-density molecular gas in the central regions of LIGs is the site of the most luminous cosmic maser sources known. The amplified main OH lines at 1667 and 1665 MHz correspond to transitions between the hyperfine splitting of a λ -doubling level at $\lambda 18 \text{ cm}$. The isotropic luminosities in the OH lines can be as strong as $\sim 10^4 L_{\odot}$, almost a million times that of the most luminous OH maser sources in the Galaxy, hence the name megamaser. Since the first detection of OH maser emission from the ULIG [Arp 220](#) ([Baan et al. 1982](#)), it became evident that this type of emission could be detected out to redshifts of $z \sim 0.5$, and therefore, that it could be used to probe the circumnuclear high-density interstellar gas in distant infrared galaxies ([Baan 1985](#), [Stavelly-Smith et al. 1987](#), [Martin et al. 1991](#), [Kazès & Baan 1991](#)). About 50 OH megamasers have now been identified ([Baan 1993](#)). The OH megamaser spectra usually exhibit broad linewidths and extended velocity wings that could be due to the rapid rotation of circumnuclear molecular disks (e.g. [Montgomery & Cohen 1992](#)), large-scale outflow motions ([Mirabel & Sanders 1987](#), [Baan 1989](#)), and/or distinct components arising in the interactive system (e.g. [Baan et al. 1992](#)).

The isotropic OH 1667 MHz luminosity is proportional to $(L_{\text{ir}})^2$ ([Martin et al. 1988](#), [Baan 1989](#)). This has been interpreted by [Baan & Haschick \(1984\)](#) as low-gain amplification of the nuclear continuum radio source by intervening OH that is being pumped by far-infrared radiation from dust. Inversion of the OH population requires a source of steep-spectrum emission in the far-infrared such as that expected from warm dust emission. Usually an OH megamaser galaxy requires a strong nuclear radio continuum source, a column density of gas along the line of sight $> 10^{22} \text{ cm}^{-2}$, a ratio $f_{60} / f_{100} \geq 0.7$, and $L_{\text{ir}} > 10^{11} L_{\odot}$ ([Mirabel & Sanders 1987](#)).

The location of megamasers in the L_{ir} versus $M(\text{H}_2)$ plane shows that they occur in objects with the largest $L_{\text{ir}} / M(\text{H}_2)$ ratios ([Mirabel & Sanders 1989](#)). At present we consider it an open question whether the origin of the far-infrared luminosity in megamasers is entirely due to star formation. A considerable fraction of the energy could ultimately come from a compact nonthermal source at the dynamical center of these galaxies. Future high-resolution VLBI observations of the OH emission may be a way to answer this question.

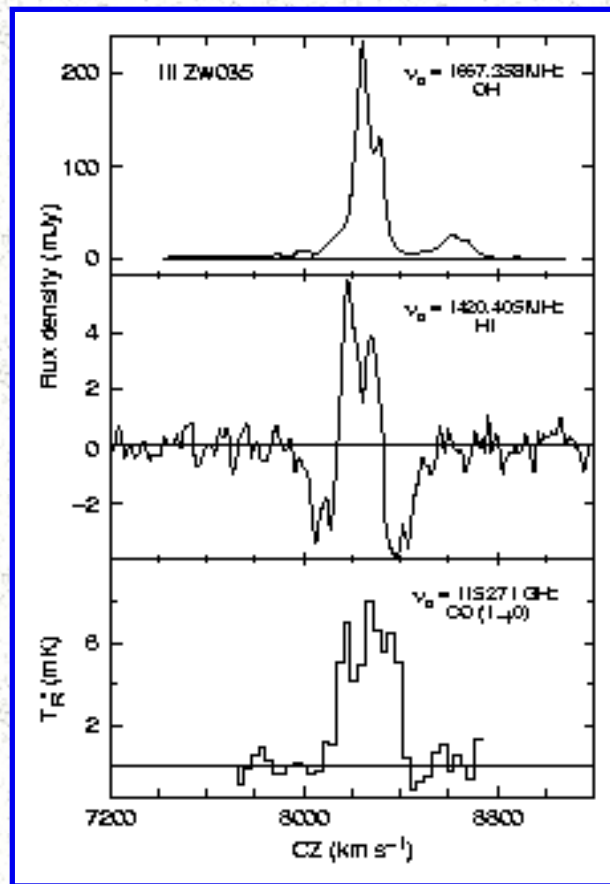


Figure 7. OH megamaser emission, H I 21-cm line emission, and CO(1- \rightarrow) line emission from the high $L_{\text{IR}}/L_{\text{B}}$ object [III Zw 35](#) ([Mirabel & Sanders 1987](#)).

There is increasing evidence that OH megamasers can eventually be used to successfully probe the molecular gas kinematics and the dynamic masses at the very centers of starburst galaxies and AGNs. Furthermore, given the observed $L_{\text{OH}} \propto L_{\text{IR}}^2$ relationship in megamaser galaxies, the spatial distribution of the far-infrared emitting region can be inferred with unprecedented angular resolution. Single-dish observations have in the past been interpreted as showing evidence for spatial extents of a few hundred parsecs in the OH emission from nearby systems ([Baan 1993](#)). However, MERLIN observations of [III Zw 35](#) have shown that most of the OH emission arises from a region only 100 pc x 60 pc in size, which is more compact than the radio continuum source ([Montgomery & Cohen 1992](#)). The velocity of the OH emission appears to trace out the characteristic signature of a rotating disk, which would imply a dynamical mass of $\sim 10^9 M_{\odot}$ inside a region of ~ 15 pc in radius.

It is interesting that one of the most compact megamasers mapped so far with MERLIN, [III Zw 35](#), is also among those megamasers with the largest implied infrared pumping efficiencies ([Mirabel & Sanders 1987](#)). [Figure 7](#) shows OH emission from [III Zw 35](#) up to 450 km s $^{-1}$ below the systemic velocity, which raises the interesting possibility of extreme circular velocities in a compact molecular torus. Similar high velocity wings, perhaps due to rapidly rotating disks, have been observed in [Mrk 231](#) and [Mrk 273](#)

([Stavely-Smith et al. 1987](#)). In addition, recent VLBI observations of [Arp 220](#) strongly suggest that the OH peak emission originates in a structure $\lesssim 1$ pc across and that nearly all of the OH emission comes from a region $\lesssim 10$ pc in size ([Lonsdale et al. 1994](#)). This would imply that the maser is physically 10-100 times smaller than previously thought ([Baan 1993](#)) and that much of the far-infrared emission from [Arp 220](#) arises in a very small region, possibly a torus surrounding a quasar nucleus. These new results suggest that OH megamasers may eventually be used to probe the central engines in AGNs, much as the H₂O megamasers have been used in [NGC 4258](#) ([Miyoshi et al. 1995](#)).

4.7 High-Energy Observations

A strong correlation has been found between the X-ray luminosity in the *Einstein* 0.2-4.5 keV energy band and the far-infrared and blue luminosities for 51 galaxies in the BGS ([David et al. 1992](#)). The best fit for the X-ray luminosity, $L_X = 9.9 \times 10^{-5} L_B + 9.3 \times 10^{-5} L_{\text{fir}}$, has two components, one proportional to L_B due to the old population (Type I supernovae and low mass X-ray binaries) and a second component proportional to L_{fir} due to young objects (Type II supernovae, O stars, high-mass binaries). LIGs with large L_{ir} / L_B ratios are dominated by the second component and can have a significant excess of X-ray flux relative to the mean (up to a factor of 10 in the case of [Arp 220](#)). It has been proposed that LIGs could make a significant contribution (up to 40%) to the X-ray background ([Griffiths & Padovani 1990](#)).

The cross-correlation between the *IRAS* PSC and the *ROSAT* All-Sky Survey (0.1-2.4 keV) allowed the identification of 244 *IRAS* galaxies that appeared to be positionally coincident with *ROSAT* X-ray sources ([Boller et al. 1992](#)). This sample is dominated by galaxies with active nuclei. An unexpected result was the discovery of a dozen spiral galaxies with X-ray luminosities up to 10^{43} erg s⁻¹, well above those found by the *Einstein* satellite. These objects have steep spectra with typical photon indexes of 2.5-3.6, which would make them preferentially detected by *ROSAT* because of its sensitivity in the soft X rays. Optical spectroscopy revealed active nuclei in half of these objects ([Boller et al. 1993](#)). In the galaxy [IRAS 15564+6359](#) a compact component can be disentangled from that of any extended component, since in the 0.1-2.4 keV energy range flux variations with a doubling time of 1500 sec (corresponding to a source size of $\lesssim 2 \times 10^{-5}$ pc) have been discovered ([Boller et al. 1994](#)). The non-detection of optical AGN activity in this galaxy is intriguing.

ROSAT observations of [Arp 220](#) reveal extended emission with $T_{\text{kin}} \sim 10^7$ K ([Heckman et al. 1996](#)), presumably due to gas ejected from the active nuclear region (see also [Section 6.4](#)). The morphology is similar to, but much more powerful than, the extended X-ray components observed in the classic starburst galaxies [NGC 253](#) and [M82](#) ([Fabbiano 1988](#)) and the edge-on spiral [NGC 3628](#) ([Fabbiano et al. 1990](#)). *ROSAT* observations of [NGC 4038/39](#) ("The Antennae") have shown that about 55% of the X-ray emission can be identified with the two galaxy nuclei plus a large ring of H II regions; the remainder appears to be diffuse emission from gas at $\sim 4 \times 10^6$ K that extends up to 30 kpc away from the merging disks ([Read et al. 1995](#)).

To test whether it is possible to use X rays to search for obscured AGN in ULIGs, as suggested by [Rieke \(1988\)](#), it is instructive to consider the case of [NGC 1068](#). Spectropolarimetry of [NGC 1068](#) by [Antonucci & Miller \(1985\)](#) revealed a Seyfert 1 nucleus hidden in a dense torus of dust and gas. Millimeter-wave observations of HCN imply $\sim 1.6 \times 10^8 M_{\odot}$ of molecular gas within a region ≈ 34 pc in radius ([Tacconi et al. 1994](#)). Assuming a spherical distribution implies a column density $\approx 5 \times 10^{24}$ atoms cm^{-2} , which - given the expected high metallicity - would produce an almost total absorption of X rays by Compton scattering. In fact, *ASCA* observations revealed that the direct component in [NGC 1068](#) is totally absorbed even at energies of 20 keV and that the observed spectrum below 20 keV is light scattered from the AGN by electrons over the absorption torus ([Ueno et al. 1994](#)). Because the central gas densities in ULIGs are likely to be even greater than in [NGC 1068](#), hard X rays most likely cannot be used to probe the central engines in these galaxies.

Gamma rays from extragalactic systems have so far mostly been detected from AGNs, either as quasi-isotropic emission from unobscured Seyferts or as beamed emission from highly variable Blazars. As expected, [NGC 1068](#) was not detected at > 20 keV ([Dermer & Gehrels 1995](#)). Observations of the nearby lower-luminosity starburst galaxies [NGC 253](#) and [M82](#), over the energy range 0.05-10 MeV, yielded a 4σ detection of [NGC 253](#) in continuum emission up to 165 keV, with an estimated luminosity of $\sim 10^{40}$ erg s^{-1} . No significant flux at high energies was detected from [M82](#) ([Bhattacharya et al. 1994](#)).

² For an L^* galaxy $M_B^* = -19.7$ mag ([Schechter 1976](#)), $M_r^* = -20.5$ mag assuming a typical $B - r = 0.75$, and $M_K^* = -24.2$ mag ([Mobasher et al. 1993](#)). [Back](#).

[Next](#)
[Contents](#)
[Previous](#)


[Next](#)
[Contents](#)
[Previous](#)

5. ORIGIN AND EVOLUTION OF LUMINOUS INFRARED GALAXIES

Table 3. *IRAS* galaxy properties versus L_{ir}

		10.5-10.99	11.0-11.49	11.5-11.99	12.0-12.50
		log ($L_{\text{ir}} / L_{\odot}$)			
No. of objects ^a		50	50	30	40
Morphology	merger	12%	32%	66%	95%
	close pair	21%	36%	14%	0%
	single (?)	67%	32%	20%	5%
Separation ^b	[kpc]	36.	27.	6.4	1.2
Opt Spectra	Seyfert 1 or 2	7%	10%	17%	34%
	LINER	28%	32%	34%	38%
	H II	65%	58%	49%	28%
$L_{\text{ir}} / L_{\text{B}}^{\text{c}}$		1	5	13	25
$L_{\text{ir}} / L'_{\text{CO}}^{\text{c}}$	$[L_{\odot} (\text{K km s}^{-1} \text{ pc}^2)^{-1}]$	37	78	122	230

^a Objects in the *IRAS* BGS plus additional ULIGs from [Kim & Sanders \(1996\)](#).

^b Mean projected separation of nuclei for mergers and close pairs only.

^c Mean values

The data presented in [Section 4](#) are sufficient to present a fairly detailed picture of the morphology of LIGs and to investigate how their properties change as a function of infrared luminosity. [Table 3](#) summarizes some of the main results using observations of the complete sample of LIGs in the BGS supplemented by data for a subsample of less luminous BGS objects and data for a larger sample of ULIGs from the survey of [Kim \(1995\)](#).

5.1 Strong Interactions and Mergers

It now seems clear that strong interactions and mergers of molecular gas-rich spirals are the trigger for producing the most luminous infrared galaxies. The images of ULIGs from the BGS (see [Figure 4](#)) show clearly that maximum infrared luminosity is produced close to the time when the two nuclei actually merge. At $L_{\text{ir}} < 10^{11} L_{\odot}$ the vast majority of infrared galaxies appear to be single, gas-rich spirals whose infrared luminosity can be accounted for largely by star formation. Over the range $L_{\text{ir}} = 10^{11}$ - $10^{12} L_{\odot}$ there is a dramatic increase in the frequency of strongly interacting systems that are extremely rich in molecular gas; at the low end of this range the luminosity appears to be dominated by starbursts with Seyferts becoming increasingly important at higher luminosities. Those objects that reach the highest infrared luminosities, $L_{\text{ir}} > 10^{12} L_{\odot}$, contain exceptionally large central concentrations of molecular gas; because of heavy dust obscuration it is hard to distinguish the relative roles of starburst and AGN activity, although the conditions are clearly optimal for fueling both enormous nuclear starbursts as well as building and/or fueling an AGN.

The enormous build-up of molecular gas in the centers of the most luminous infrared objects plays a fundamental role in LIGs and is best illustrated by showing data for several relatively nearby well-studied objects. The ultimate fate of these mergers, once their infrared excess subsides, is not completely clear. Examples are also shown below for a small but important subclass of objects which show both strong optical and infrared emission, and which plausibly represent a transition stage in the evolution of LIGs into optically selected AGN (e.g. [Sanders et al. 1988b](#)). Finally we mention a few objects initially identified as HyLIGs that illustrate why caution needs to be taken when identifying objects at higher- z .

5.2 Case Studies

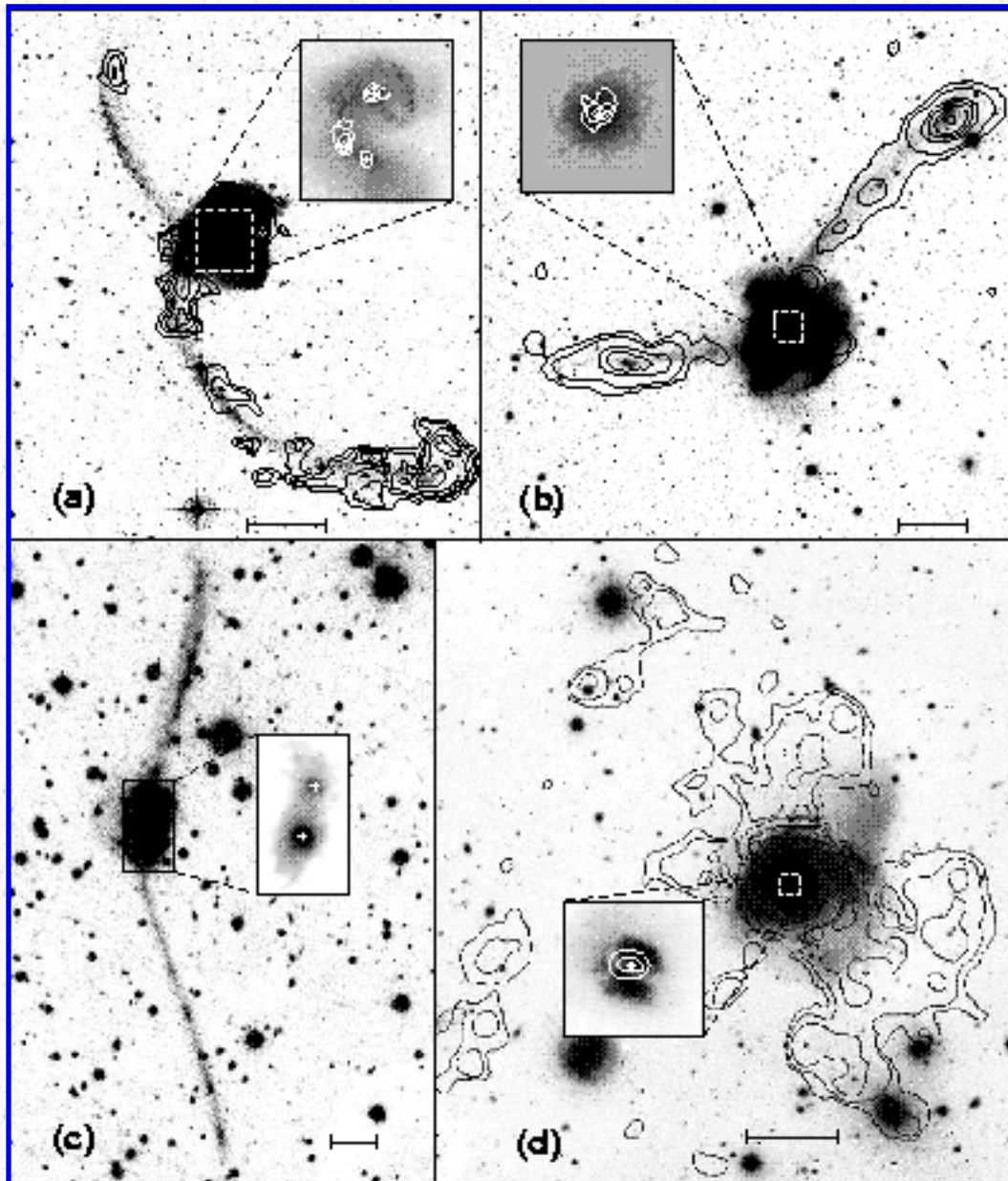


Figure 8. Well-studied mergers: (a) [NGC 4038 / 39](#) ([Arp 244](#) = "The Antennae"); (b) [NGC 7252](#) ([Arp 226](#) = "Atoms for Peace"); (c) [IRAS 19254-7245](#) ("The Super Antennae"); (d) [IC 4553 / 54](#) ([Arp 220](#)). Contours of H I 21-cm line column density (black) are superimposed on deep optical (*r*-band) images. Inserts show a more detailed view in the *K*-band ($2.2 \mu\text{m}$) of the nuclear regions of [NGC 4038 / 39](#), [NGC 7252](#), and [IRAS 19254-7245](#), and in the *r*-band ($0.65 \mu\text{m}$) of [Arp 220](#). White contours represent the CO(1 \rightarrow 0) line integrated intensity as measured by the OVRO millimeter-wave interferometer. No H I or CO interferometer data are available for the southern hemisphere object [IRAS 19254-7245](#). The scale bar represents 20 kpc.

5.2.1 MERGERS OF MOLECULAR GAS-RICH SPIRALS [NGC 4038 / 39](#) ([Arp 244](#) = [VV 245](#) = "The Antennae") This classic, nearby "early merger" system is composed of what appear to be two overlapping, distorted, late-type spiral disks ([Figure 8a](#)). The total infrared luminosity is the minimum

required by our definition of LIG. The K -band image shows two nuclei ~ 15 kpc apart and what appears to be a large ring of bright H II regions in the northern disk. CO interferometer observations ([Stanford et al. 1990](#)) show that $\sim 60\%$ of the $3.9 \times 10^9 M_{\odot}$ of molecular gas in the system ([Sanders & Mirabel 1985](#), [Young et al. 1995](#)) is concentrated in the two nuclei and in a large off-nuclear complex where the two disks strongly overlap. No CO has been detected in the extended tails. In contrast, about 70% of the total H I mass, $M(\text{H I}) \sim 10^9 M_{\odot}$, is associated with the long (total extent of ~ 100 kpc) tidal tails (van der Hulst et al., in preparation). About one quarter of the total H I mass is located at the tip of the southern "antenna". In this early merger the total ratio $M(\text{H}_2) / M(\text{H I})$ is ~ 4 .

[NGC 7252](#) (*Arp 226* = "Atoms for Peace") [NGC 7252](#) has been considered the prototype of a late-stage merger ([Schweizer 1978](#)). This object has $L_{\text{IR}} \sim 5 \times 10^{10} L_{\odot}$ and therefore is currently not a LIG. The K -band image shows a single nucleus inside what has been described as a relaxed elliptical body. The optical image shows relatively large symmetric tails, which rotate in opposite directions and have a total extent of ~ 130 kpc ([Figure 8b](#)). [NGC 7252](#) has been described as a decaying merger of two massive gas-rich late-type spirals caught in the act of forming a single elliptical galaxy ([Schweizer 1978](#), [Casoli et al. 1991](#), [Fritze-von Alvensleben & Gerhard 1994](#)). However, it is not yet clear whether this system has passed through a LIG phase. Single-dish ([Dupraz et al. 1990](#)) and interferometer ([Wang et al. 1992](#)) CO observations reveal a nuclear molecular gas disk at $r < 1.5$ kpc, which contains nearly 75% of the total H_2 mass of $4.7 \times 10^9 M_{\odot}$. [Hibbard et al. \(1994\)](#) and [Hibbard & van Gorkom \(1996\)](#) detect a slightly smaller total mass of H I ($3.6 \times 10^9 M_{\odot}$), but *all* of the H I is located in the tidal tails. Until most of the H I and H_2 is either consumed, expelled, or ionized, it would appear that [NGC 7252](#) still has too much cold gas to resemble most present-day ellipticals.

[IRAS 19254-7245](#) ("The Super Antennae") [IRAS 19254-7245](#) is a remarkable ULIG in which two distinct rotating merging disks can still be identified ([Mirabel et al. 1991](#)). The colossal tidal tails have a total extent of ~ 350 kpc ([Figure 8c](#)). Among the 20 ULIGs in the *IRAS* BGS this object has the largest projected nuclear separation (~ 10 kpc; [Melnick & Mirabel 1990](#)). If the *IRAS* luminosity has the same spatial distribution as the observed $10\text{-}\mu\text{m}$ luminosity, then $\gtrsim 80\%$ of the total luminosity, $L_{\text{IR}} = 1.1 \times 10^{12} L_{\odot}$, originates in the southern, heavily obscured Seyfert nucleus. The total molecular gas content of the system is $M(\text{H}_2) \sim 3.0 \times 10^{10} M_{\odot}$ ([Mirabel et al. 1988](#)).

[IC 4553 / 54](#) (*Arp 220*) At a distance of 77 Mpc, [Arp 220](#) is the nearest ULIG (by a factor of ~ 2). In contrast to "The Super Antennae", it shows two relatively short and wide tails ([Figure 8d](#)). The nuclear region is completely obscured in the optical, but two distinct nuclei separated by $0.8''$ (~ 300 pc) are detected at K -band ([Graham et al. 1990](#)). The radial brightness profile at $2.2 \mu\text{m}$ is closely approximated by a $r^{-1/4}$ de Vaucouleurs' profile ([Wright et al. 1990](#), [Kim 1995](#)). The total mass of molecular gas is $M(\text{H}_2) \sim 3.6 \times 10^{10} M_{\odot}$, with $\sim 2/3$ of it inside a projected radius of ~ 300 pc. Compact OH megamaser emission ($\lesssim 10$ pc in diameter) has recently been discovered at the center of [Arp 220](#) ([Lonsdale et al. 1994](#)). H I is detected in absorption against the nuclear radio continuum source ([Mirabel 1982](#)). In

emission, all of the $\sim 2.3 \times 10^9 M_{\odot}$ of H I is located outside the main body ([Hibbard & Yun 1996](#)). Although as luminous as "The Super Antennae", the shorter tidal tails, smaller nuclear separation, and more relaxed central body of [Arp 220](#) suggest that it is a more advanced merger. Because of the strong H I absorption it is not possible to estimate the total mass of H I in the merger disks; however, most of the cold gas there is likely to be in molecular form, and the overall ratio $M(\text{H}_2) / M(\text{H I})$ is probably close to 15.

5.2.2 ENCOUNTERS IN CLUSTERS Most LIGs detected by *IRAS* appear to involve strong interactions/mergers of molecular gas-rich spirals where the pairs are either isolated or part of small groups. In these interactions/mergers the relative mean velocity of the individual members is typically $\approx 200 \text{ km s}^{-1}$. These conditions are not expected to be typical of cluster environments where the relative velocities are often much higher, and many galaxies may be either gas-poor spirals (from ram-pressure stripping) or already transformed into ellipticals (perhaps due to past mergers). Although multiple high-speed encounters in clusters may produce some LIGs (e.g. [Moore et al. 1996](#)), the relatively small number of *IRAS* LIGs found in clusters suggests that lower-speed mergers in pairs or loose groups may be a more efficient way of enhancing infrared activity. As examples of the types of strong interactions involving relatively large ($\gtrsim L^*$) galaxies in low- z clusters, we discuss here observations of an elliptical-spiral encounter ([Arp 105](#)) and a relatively high-speed lenticular-spiral encounter (NGC 5291A/B).

[Arp 105](#) ([Figure 9a](#)) consists of an infrared luminous ($L_{\text{ir}} \sim 10^{11} L_{\odot}$) spiral galaxy (NGC 3561A) being torn apart by a massive elliptical (NGC 3561B) in the X-ray rich cluster [Abell 1185](#). [Duc & Mirabel \(1994\)](#) find that the elliptical has already accreted gas-rich objects and may be the precursor of a cD galaxy. At the tip of one of the colossal tidal tails that emanate from the spiral are a compact dwarf galaxy and an irregular galaxy of Magellanic type. The H I and CO interferometer observations by [Duc \(1995\)](#) show that the collision has caused a marked spatial separation of the cold interstellar gas: Whereas all of the $\sim 10^{10} M_{\odot}$ of molecular gas (H_2) is found within the central $\sim 6 \text{ kpc}$ radius of the spiral, a similar mass of atomic gas (H I) is found outside that region, most of it far from the spiral galaxy near the tips of the tidal tails. H I clouds infalling at high velocities toward the nucleus of the elliptical are detected in absorption against a central compact radio source.

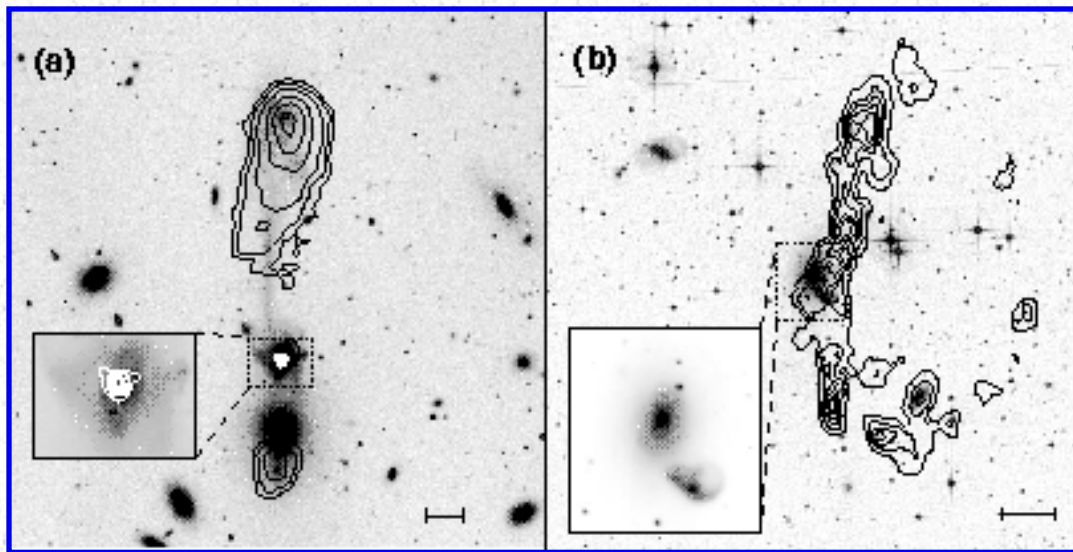


Figure 9. Encounters in clusters: (a) NGC 3561A/B ([Arp 105](#)); (b) NGC 5291A/B ("Sea shell"). Contours of H I 21-cm line column density (*black*) are superimposed on deep optical (*r*-band) images. Inserts show a more detailed view in *r*-band of the spiral galaxy NGC 3561A ([Duc & Mirabel 1994](#)), and of the interacting pair NGC 5291A/B. White contours represent the CO(1→0) line integrated intensity as measured by the IRAM millimeter-wave interferometer. CO emission has not been detected in NGC 5291A/B. The scale bar represents 20 kpc.

[Figure 9b](#) shows an optical image of NGC 5291A/B ([Duc & Mirabel 1996](#), in preparation) and H I column density map ([Malphrus et al. 1996](#), in preparation). The nuclei of the lenticular galaxy NGC 5291A and the spiral NGC 5291B (the "Sea shell" galaxy) are at a projected separation of 12 kpc and are moving with a relative radial speed of $\sim 450 \text{ km s}^{-1}$ ([Longmore et al. 1979](#)). [Figure 9b](#) reveals a multitude of intergalactic H II regions superimposed on an arc-like distribution of H I, which has a diameter of ~ 200 kpc and a total H I mass of $\sim 10^{11} M_{\odot}$ ([Simpson et al.](#), private communication). However, optical spectroscopy of the spiral that is being torn apart shows no signs of recent star formation, which is consistent with its apparently low infrared luminosity ($L_{\text{IR}} < 10^9 L_{\odot}$); this source was not detected by *IRAS*.

5.2.3 MOLECULAR GAS-RICH MERGERS IN QSOs AND PRGs Infrared and millimeter-wave observations of QSOs and PRGs show that a significant fraction of these objects have values of L_{IR} and $M(\text{H}_2)$ that overlap values found for infrared-selected ULIGs. These data have been used as evidence for an evolutionary connection between QSOs, PRGs, and ULIGs (e.g. [Sanders et al. 1988b](#), [Mirabel et al. 1989](#)). [Figure 10](#) shows high-resolution optical images of the optically-selected QSO [Mrk 1014](#), the radio-selected PRG [Pks 1345+12](#), and the radio-selected QSO [3C 48](#), three objects that exhibit several properties in common with ULIGs.

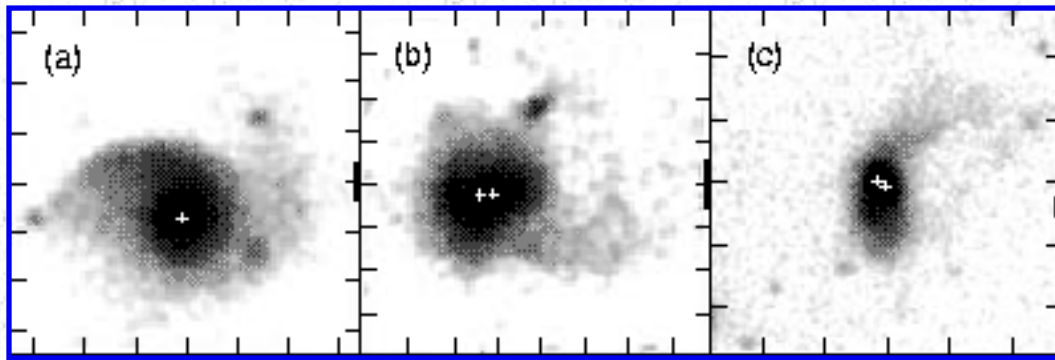


Figure 10. Optical images of QSOs and PRGs with strong infrared emission: (a) [Mrk 1014 \(PG 0157+001\)](#), (b) [4C 12.50 \(Pks 1345+12\)](#), (c) [3C 48](#). The "+" sign indicates the position of putative optical nuclei. Tick marks are at 5" intervals, and the scale bar represents 10 kpc.

[Figure 10a](#) shows the UV-excess QSO [Mrk 1014](#) at a redshift of 0.163. The deep CCD image shows two tidal tails extending from a large distorted disk with a total diameter of ~ 90 kpc (e.g. [Mackenty & Stockton 1984](#)). This warm infrared object has $L_{\text{ir}} \sim 3 \times 10^{12} L_{\odot}$ and $M(\text{H}_2) \sim 4 \times 10^{10} M_{\odot}$ ([Sanders et al. 1988c](#)).

[Figure 10b](#) shows a deep optical image of the PRG [4C 12.50](#). This object exhibits a double nucleus embedded in a distorted disk ~ 85 kpc in diameter (see also [Heckman et al. 1986](#)). *IRAS* observations imply $L_{\text{ir}} \sim 1.6 \times 10^{12} L_{\odot}$. CO emission ([Mirabel et al. 1989](#)) and H I absorption ([Mirabel 1989](#)) with widths of $\sim 950 \text{ km s}^{-1}$ have been detected from this object. The CO data implies an extremely large mass of molecular gas, $M(\text{H}_2) \sim 6.5 \times 10^{10} M_{\odot}$. [Mirabel \(1989\)](#) proposed that objects like [4C 12.50](#) (which is classified as a compact steep-spectrum radio source) are relatively young PRGs that have evolved from progenitors like [Arp 220](#), where a powerful compact source of nonthermal radio emission is still confined by a large nuclear concentration of gas and dust.

[Figure 10c](#) shows a recent deep optical image of [3C 48](#), the first radio source to be identified as a QSO ([Matthews & Sandage 1963](#)) and the second QSO to have its redshift determined ([Greenstein & Matthews 1963](#)). [3C 48](#) appears to have a double nucleus and at least one prominent tidal tail ([Stockton & Ridgway 1991](#)). [Neugebauer et al. \(1985\)](#) used the strength and shape of the far-infrared continuum, and [Stein \(1995\)](#) used the f_{60} / f_{25} ratio versus the radio spectral index at 4.8 GHz to argue that the dominant luminosity source in this classic QSO is star formation in the host galaxy rather than the central AGN. *IRAS* observations of [3C 48](#) imply $L_{\text{ir}} \sim 5 \times 10^{12} L_{\odot}$, and the recent detection of CO emission by [Scoville et al. \(1993\)](#) implies a molecular gas mass $M(\text{H}_2) \sim 4 \times 10^{10} M_{\odot}$ (see also [Evans et al. 1996b](#)).

5.2.4 GRAVITATIONAL LENSING IN HIGH-Z OBJECTS The identification of the *IRAS* Faint Source 10214+4724 with an emission-line galaxy at a redshift of 2.286 ([Rowan-Robinson et al. 1991](#)) has attracted considerable interest. The apparent enormous infrared luminosity, $L_{\text{ir}} \sim 2 \times 10^{14} L_{\odot}$, the

detection of $\sim 10^{11} M_{\odot}$ of molecular gas ([Brown & Vanden Bout 1991](#); [Solomon et al. 1992b, c](#); [Radford et al. 1996](#)), and the detection of strong submillimeter continuum emission from dust ([Clements et al. 1992](#), [Downes et al. 1992](#)) led many observers to propose that this object was a prime candidate for a "primeval galaxy". However, IRAS 10214+4724 exhibits at least one unusual property for an object with such extreme luminosity and mass; the CO line width of $\sim 250 \text{ km s}^{-1}$ is small for such a massive object.

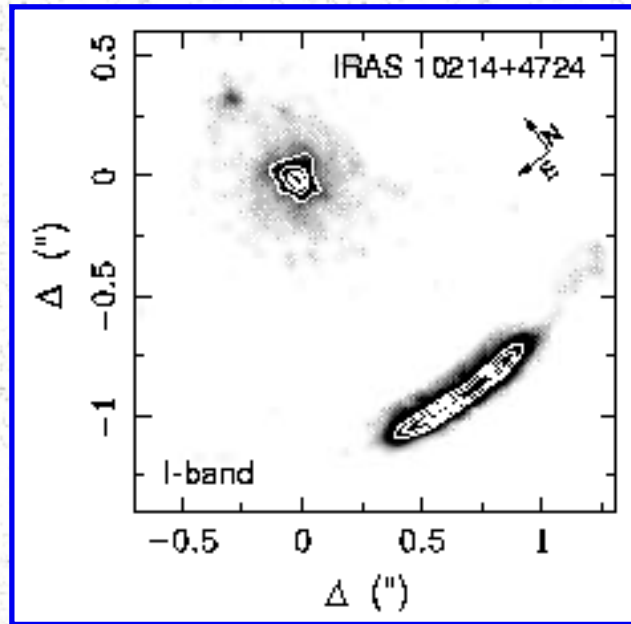


Figure 11. *HST* Planetary Camera (F814W) image of the gravitational lens object IRAS 10214+4724 ([Eisenhart et al. 1996](#)).

The idea that IRAS 10214+4724 might be gravitationally lensed by a foreground galaxy or group of galaxies ([Elston et al. 1994](#), [Trentham 1995](#), [Broadhurst & Lehár 1995](#)) gained support from sub-arcsecond *K*-band images obtained with the Keck telescope ([Matthews et al. 1994](#), [Graham & Liu 1995](#)), and now appears certain from the image obtained with the *Hubble Space Telescope* (*HST*) ([Figure 11](#)). The geometry of the lensed arc suggests an amplification factor of ~ 30 for the infrared emission ([Eisenhart et al. 1996](#)). CO interferometer maps indicate that the molecular gas may be somewhat more extended than the infrared emission ([Scoville et al. 1995](#), [Downes et al. 1995](#)), and [Downes et al. \(1995\)](#) suggest that the CO may be amplified by a factor $\lesssim 10$. Thus, the intrinsic infrared luminosity and molecular gas mass of this object may only be $L_{\text{ir}} \sim 7 \times 10^{12} L_{\odot}$ and $M(\text{H}_2) \sim 2 \times 10^{10} M_{\odot}$, respectively, suggesting that IRAS 10214+4724 is not a unique infrared selected object but is better described as a high-redshift analogue of ULIGs found in the local Universe.

At present, the only other *IRAS* object at $z > 2$ that has been detected in CO is the Cloverleaf QSO at $z \sim 2.5$, which is also a lensed object ([Barvainis et al. 1994](#)). After correcting for amplification, the Cloverleaf appears to have a similar infrared and submillimeter spectrum as for IRAS 10214+4724 ([Barvainis et al. 1995](#)), again suggesting that this object is yet another high-redshift analog of local ULIGs.

However, several objects at $z > 4$ not detected by *IRAS* have recently been shown to be strong far-infrared (rest-frame) emitters ([Omont et al. 1996a](#)), and one of these sources - the radio-quiet QSO [BR1202-0725](#) at $z = 4.69$ ([Irwin et al. 1991](#)) - was recently detected in CO ([Ohta et al. 1996](#), [Omont et al. 1996b](#)) implying $M(\text{H}_2) \sim 6 \times 10^{10} M_{\odot}$. This object has been shown to have a submillimeter spectrum remarkably similar to IRAS 10214+4724 ([McMahon et al. 1994](#), [Isaak et al. 1994](#)). An *HST* image ([Hu et al. 1996](#)) shows no obvious evidence that this object is lensed, but it may be premature to rule out this possibility.

If one extrapolates the local luminosity function of ULIGs assuming relatively strong evolution (e.g. [Kim & Sanders 1996](#)), then the probability that a ULIG detected at $z \gtrsim 2$ is lensed by at least a factor of 10 can be as high as $\sim 30\%$ ([Trentham 1995](#), [Broadhurst & Lehar 1995](#)). Future studies of LIGs at high redshifts will almost certainly require high-resolution imaging to test whether these objects are lensed.

[Next](#)[Contents](#)[Previous](#)

[Next](#)[Contents](#)[Previous](#)

6. ASSOCIATED PHENOMENA

6.1 *Formation of Ellipticals*

In disk-disk collisions of galaxies, dynamical friction and subsequent relaxation may produce a mass distribution similar to that in classic elliptical galaxies. From the relative numbers of mergers and ellipticals in the New General Catalogue [Toomre \(1977\)](#) estimated that a large fraction of ellipticals could be formed via merging. The first direct observational evidence for the transition from a disk-disk merger toward an elliptical was presented in the optical study of [NGC 7252](#) by [Schweizer \(1982\)](#). The brightness distribution over most of the main body of this galaxy is closely approximated by a de Vacouleurs ($r^{-1/4}$) profile. However, [NGC 7252](#) still contains large amounts of interstellar gas and exhibits a pair of prominent tidal tails (see [Figure 9b](#)); neither property is typical of ellipticals.

Near-infrared images are less effected by dust extinction and also provide a better probe of the older stellar population, which contains most of the disk mass and therefore determines the gravitational potential. *K*-band images of six mergers by [Wright et al. \(1990\)](#) showed that the infrared radial brightness profiles for two LIGs - [Arp 220](#) and [NGC 2623](#) - follow an $r^{-1/4}$ law over most of the observable disks. Among eight merger remnants, [Stanford & Bushouse \(1991\)](#) found *K*-band brightness profiles for four objects that were well fitted by an $r^{-1/4}$ law over most of the observable disks. [Kim \(1995\)](#) finds a similar proportion ($\sim 50\%$) of ULIGs whose *K*-band profiles are well fit by a $r^{-1/4}$ law.

More recently, [Kormendy & Sanders \(1992\)](#) have proposed that ULIGs are elliptical galaxies forming by merger-induced dissipative collapse. The extremely large central gas densities ($\sim 10^2\text{-}10^3 M_{\odot} \text{pc}^{-3}$) observed in many nearby ULIGs (see [Section 4.6.2](#)) and the large stellar velocity dispersions found in the nuclei of [Arp 220](#) and [NGC 6240](#) ([Doyon et al. 1994](#)) are comparable to the stellar densities and velocity dispersions respectively, in the central compact cores of ellipticals.

Despite the *K*-band and CO evidence that LIGs may be forming ellipticals, we still need to account for two important additional properties of ellipticals: 1. the large population of globular clusters in the extended halos of elliptical galaxies, which cannot be accounted for by the sum of globulars in two preexisting spirals ([van den Bergh 1990](#)), and 2. the need to remove the large amounts of cold gas and dust present in infrared-luminous mergers in order to approximate the relative gas-poor properties of ellipticals. These two issues are addressed below.

6.2 Formation of Star Clusters

Populations of bright blue pointlike objects have recently been discovered with *HST* in the galaxy at the center of the Perseus cluster, [NGC 1275 \(Holtzman et al. 1992\)](#), and in the disk-disk mergers [NGC 7252 \(Whitmore et al. 1993\)](#), "[The Antennae](#)" ([Whitmore & Schweizer 1995](#)), and [Arp 299 \(Meurer et al. 1995, Vacca 1996\)](#). These objects have $M_V \sim -11$ to -16 , and it has been proposed that they are young clusters that are, or may evolve into, globular clusters. If this hypothesis is true, then the number of globular clusters would indeed increase during the merger of gas-rich spirals, thus weakening one of the main arguments against ellipticals being formed through disk mergers.

The interpretation of these star clusters as protoglobulars has been questioned by van den Bergh ([1995a, b](#)), who argues that mergers simply increase the rate of normal star and cluster formation and do not promote a specific population of very massive clusters that will evolve into globulars. In fact, the luminosity function of the blue clusters in [The Antennae](#) has a power-law shape as do open clusters in the Milky Way, rather than the Gaussian shape of the luminosity function of globular clusters ([Whitmore & Schweizer 1995, van den Bergh 1995b](#); but see [Meurer 1995](#)). Furthermore, the light radii of the young clusters in [The Antennae](#) seem to be larger than in typical globular clusters by a factor of about three. Future observations of these objects with corrected *HST* optics may provide better images that can prove if these blue clusters indeed have the star densities typical of globulars.

6.3 Formation of Dwarf Galaxies

Collisions between giant disk galaxies may trigger the formation of dwarf galaxies. This idea, which was first proposed by [Zwicky \(1956\)](#) and later by [Schweizer \(1978\)](#), has received recent observational support ([Mirabel et al. 1991, 1992](#); [Elmegreen et al. 1993](#); [Duc & Mirabel 1994](#)). Renewed interest in this phenomenon arose from the inspection of the optical images of ULIGs, which frequently exhibit patches of optically emitting material along the tidal tails (see [Figures 8a, b, c](#)). These objects appear to become bluer near the tips of the tails at the position of massive clouds of H I. These condensations have a wide range of absolute magnitudes, $M_V \sim -14$ to -19.2 , and H I masses, $M(\text{H I}) \sim 5 \times 10^8$ to $6 \times 10^9 M_\odot$. [Mirabel et al. \(1995\)](#) have shown that objects resembling irregular dwarfs, blue compacts, and irregulars of Magellanic type are formed in the tails. These small galaxies of tidal origin are likely to become detached systems, namely, isolated dwarf galaxies. Because the matter out of which they are formed has been removed from the outer parts of giant disk galaxies, the tidal dwarfs we observe forming today have a metallicity of about one third solar ([Duc 1995](#)).

It is interesting that in these recycled galaxies of tidal origin there is - as in globular clusters - no compelling evidence for dark matter ([Mirabel et al. 1995](#)). The true fraction of dwarf galaxies that may have been formed by processes similar to the tidal interactions we observe today between giant spiral galaxies will require more extensive observations of interacting systems. A recent step forward is the

statistical finding that perhaps as much as one half of the dwarf population in groups is the product of interactions among the parent galaxies ([Hunsberger et al. 1996](#)).

6.4 *Enrichment of the Intergalactic Medium*

X-Ray and optical evidence for galactic superwinds has been presented for both ULIGs and PRGs ([Heckman et al. 1990, 1996](#); [Veilleux et al. 1995](#)). In these objects, it has been proposed that the combined kinetic energy from supernovae and stellar winds from powerful nuclear starbursts drive large-scale outflows that shock, heat, and accelerate the circumnuclear ambient gas. The morphology, kinematics, and physical properties of the optically emitting gas tend to support this model. Continuum-subtracted narrow-band images show emission-line nebulosity extending over tens of kiloparsecs; a good example of this phenomenon is the enormous H α bubble found in [Arp 220](#) ([Armus et al. 1987](#)). Further kinematic signatures of outflows along a galaxy's minor axis are provided by observed double emission-line profiles with line splittings of 200-600 km s⁻¹; a spectacular example is the \gtrsim 1500 km s⁻¹ splitting found in the nuclear superbubble of NGC 3079 ([Veilleux et al. 1994](#)). Additional evidence for mass outflows in LIGs includes the statistical difference found between the H I 21-cm line and optical emission line redshifts. This difference is likely due to outflow motions of the optical line-emitting gas ([Mirabel & Sanders 1988](#)).

Galactic superwinds may play an important role in the metal enrichment of the intergalactic medium. [Heckman et al. \(1990\)](#) calculate a mass loss rate, $dM/dt = 4 (L_{\text{fir}, 11} M_{\odot} \text{ year}^{-1})$, where $L_{\text{fir}, 11}$ is the far-infrared luminosity in units of $10^{11} L_{\odot}$, implying that a galaxy like [Arp 220](#) can be expected to inject $\sim 5 \times 10^8 M_{\odot}$ of metals and $\sim 10^{58}$ ergs over an estimated lifetime of $\sim 10^7$ years. Assuming no cosmological evolution and using a luminosity function for *IRAS* galaxies similar to that given in [Figure 1](#), [Heckman et al. \(1990\)](#) derived a total mass-injection rate of $\sim 2 \times 10^7 (M_{\odot} \text{ Mpc}^{-3})$, 25% of which is in metals. If cosmological evolution is included (see [Section 3.1](#)), then the injected mass and energy can increase by an order of magnitude.

The superwinds observed in nearby ULIGs may provide local examples that can be used to understand the X-ray iron abundance of $\sim 1/3$ solar in the intracluster medium ([Arnaud et al. 1992](#)). Recent *ASCA* observations of large amounts of silicon and oxygen in four nearby clusters indicate that type II supernovae are responsible for the metal enrichment ([Loewenstein & Mushotzky 1996](#)). In turn, the metals found in nearby clusters may represent the fossil records of ancient starbursts ([Elbaz et al. 1992](#), [Terlevich & Boyle 1993](#)). More specifically, the iron-elliptical correlation observed in clusters may suggest that giant ellipticals indeed went through an ULIG-superwind phase.

On the question of the impact that these galactic superwinds may have on the interstellar gas content of the host galaxy, it is important to know the fraction of the total interstellar gas that these winds can entrain and expel into the intergalactic medium. [Heckman et al. \(1990\)](#) suggest that the maximum amount of ambient material ejected by the wind is $M_{\text{ej,max}} = 10^{10} (E_{\text{wind}} / 10^{58}) M_{\odot}$, which implies that

when the entrained material has velocities above the escape velocity of the host galaxy, the entire interstellar medium could be blown away. Since the observed velocities of the line-emitting gas in LIGs are close to the escape velocities, it appears possible that a large fraction of the interstellar gas may be driven out of the host galaxy, and that in some cases the entire neutral interstellar medium may have been lost, as appears to be the case in most giant ellipticals.

[Next](#)

[Contents](#)

[Previous](#)

[Next](#)[Contents](#)[Previous](#)

7. THEORETICAL MODELS

Recent theoretical models have been quite successful in explaining several important features that appear to be common to most gas-rich mergers. For example, theorists reacted rapidly to the observational discovery of high concentrations of cold gas in the central regions of some mergers and developed new dynamic models with gas+stars that have provided much needed insight into how such gas concentrations are produced (e.g. [Barnes & Hernquist 1992](#), [Barnes 1995](#)). During collisions, the gas readily loses angular momentum due to dynamical friction, decouples from the stars, and inflows rapidly toward the merger nuclei. The typical half-mass radius of the gas is only 2.5% that of the stars, which scaled to Milky Way units implies $\sim 5 \times 10^9 M_{\odot}$ of neutral gas within a radius of ~ 140 pc and a gas density of $\sim 10^3 M_{\odot} \text{pc}^{-3}$ (Barnes 1995).

Although all gas-rich disk-disk mergers appear to end up with enormous gas densities at their centers, independent of the specific orbital parameters, the rate of gas inflow may depend on the structure of the progenitor galaxies, specifically, on the size of a dense central bulge ([Mihos & Hernquist 1994](#)). Galaxies without bulges develop bars that produce a more steady inflow that may last $\sim 1.5 \times 10^8$ years. By contrast, in objects with large bulges the disk tends to be stabilized against strong inflow until just before the galaxies finally coalesce, when strong dissipation finally drives the contained gas to the center in $\lesssim 5 \times 10^7$ years. If the level of infrared activity depends on the *rate* of gas infall into what is to be the maximum central gas density configuration, or if some other mechanism such as a binary black hole is required to create an extreme nuclear starburst (e.g. [Taniguchi & Wada 1996](#)), then it may be the case that not all mergers of gas-rich spirals will produce ULIGs.

Noninteracting spirals typically have large quantities of H I beyond their optical disks. For instance, in the Milky Way most of the H I mass is beyond the solar circle, whereas most of the molecular gas is at galactocentric radii $< 0.7 R_{\odot}$. Computer models predict that a large fraction of the H I gas in the outer regions of the pre-encounter disks will be pulled out to large radii in the form of tidal tails, out of which dwarf irregular galaxies can be formed ([Barnes & Hernquist 1992](#), [Elmegreen 1993](#)). [Elmegreen et al. \(1993\)](#) have proposed that the heating of the interstellar medium due to the encounter increases the Jeans' mass and that the H I gas that leads the matter launched into intergalactic space will form self-gravitationally bound cloud complexes, which may collapse and appear as detached irregular dwarf galaxies. This model forms large H I clouds with masses as large as $10^9 M_{\odot}$ at the end of the tidal tails opposite the companion ([Mirabel et al. 1992](#), [Duc & Mirabel 1994](#)). In the [Barnes & Hernquist \(1992\)](#) model, however, the clumps form from collapse of the stellar population, with mass fluctuations on all

scales, producing also "failed dwarfs" of only old stars due to the fact that the potential wells are too shallow to capture enough H I to form new stars. This result is consistent with the wide range of $B - V$ colors of the condensations along the tidal tails of some ULIGs ([Mirabel et al. 1991](#)).

[Next](#)

[Contents](#)

[Previous](#)

[Next](#)[Contents](#)[Previous](#)

8. SUMMARY

Our knowledge of luminous galaxies has increased dramatically as a result of the *IRAS* all-sky survey. During the past decade, ground-based redshift surveys have succeeded in identifying thousands of LIGs, including several hundred ULIGs in the local Universe ($z \lesssim 0.3$), and detailed multiwavelength studies, particularly of the brightest objects, have provided substantial information on what types of galaxies emit these large infrared luminosities. It seems clear that strong interactions/mergers of gas-rich spirals are responsible for the great majority of LIGs and that enormous starbursts must be involved in generating a substantial fraction of the infrared luminosity, at least in the early phases of the interaction.

Theoretical models have added substantially to our understanding of the merger process, in particular by showing how it is possible to build up enormous concentrations of gas in the centers of the merger remnant. Interferometer measurements at millimeter wavelengths show that the most luminous infrared objects often contain as much as $10^{10} M_{\odot}$ of gas within 0.5-kpc radius of the merger nucleus! Such enormous gas concentrations are an ideal breeding ground for a variety of powerful phenomena, including powerful starbursts with their accompanying superwinds that may add substantially to the metal enrichment of the intergalactic medium, the formation of massive star clusters, and most likely the building and/or fueling of an AGN. LIGs very likely represent an important link between starburst galaxies and the AGN phenomena exhibited by QSOs and PRGs. They also likely represent transition objects spanning the gap between merging spirals and emerging ellipticals.

Future infrared space missions and more sensitive ground-based submillimeter surveys will succeed in identifying more distant LIGs, thus allowing a test of whether the infrared luminosity function evolves as steeply as that of QSOs and whether LIGs were more numerous in clusters during the epoch when it is presumed that most of the ellipticals were formed from mergers of spirals.

However, detailed studies of objects already identified from the *IRAS* survey will probably play the largest role in our ability to determine the nature of the dominant energy sources in LIGs and to understand more precisely what parameters lead to the origin and ultimate fate of these objects. The following research areas could prove particularly productive:

1. Detailed multiwavelength studies of those LIGs already identified in the *IRAS* BGS that do not show obvious evidence of current or past interactions (e.g. [IRAS 10173+0828](#), [VII Zw 031](#)). Do these "exceptions" to the merger hypothesis simply represent the end-stage of the merger after most of the obvious tidal features have disappeared, or do they represent an alternative way of producing LIGs ?
2. Identification of more "transition objects" - those galaxies that are currently LIGs but that also show broad Sy 1 emission lines or powerful radio cores/jets that are characteristics of QSOs and PRGs respectively. These objects currently represent ~ 15% of LIGs in the *IRAS* BGS and many more should be discovered in follow-up studies of sources in existing catalogs of fainter objects.
3. A systematic search for possible fossil remnants of the ULIG merger phase (e.g. molecular gas, faint tidal features, etc.) in the host galaxies of QSOs and PRGs.
4. Mid- and far-infrared spectroscopy with the *Infrared Space Observatory (ISO)* to better study the nature of the deeply embedded energy sources in LIGs.
5. More elaborate theoretical models that include a better treatment of star formation, stellar winds, and supernovae explosions to better follow the evolution and fate of the central gas concentration.
6. VLBI observations of extragalactic OH megamasers - ULIGs host a class of megamasers that may prove to be a powerful dynamical probe that can be used to test for the presence of supermassive black holes.

Finally, it should eventually be possible to better discriminate between AGN versus starbursts in ULIGs by direct measurement of the size of the emitting region at mid- and far-infrared wavelengths. This could happen in the next few years as ground-based submillimeter interferometers come into operation and later with proposed airborne and space-based platforms such as *SOFIA* and *FIRST*.

ACKNOWLEDGMENTS

It is a pleasure to thank the many people who sent us preprints and reprints of their work on luminous infrared galaxies. We also thank L. Armus, M. Arnaud, W. Baan, J. Ballet, J. Barnes, E. Brinks, R. Cohen, L. Cowie, P. Duc, A. Evans, T. Heckman, E. Hu, R. Joseph, J. Kormendy, J. Mazzarella, R. Norris, T. Soifer, A. Stockton, N. Trentham, W. Vacca, and S. Veilleux for helpful discussions and comments while writing the manuscript. We are grateful to those people who generously made their HI data available to us for use in constructing overlays for the figures: E. Brinks ([Figure 9a](#)), C. Simpson and S. Gottesman ([Figure 9b](#)), J. Hibbard ([Figures 8b](#) and [8d](#)), J. van der Hulst ([Figure 8a](#)); to P Bryant for permission to use his new millimeter-wave interferometer CO data in [Figure 6d](#); to J. Wink for permission to use the CO map in [Figure 9a](#); to A. Stockton for permission to reproduce optical images obtained with the [CFHT](#) and the [UH 2.2-m telescope](#) ([Figure 10](#)); and to P. Eisenhart for permission to use the *HST* image reproduced in [Figure 11](#). We would particularly like to express our appreciation to Pierre-Alain Duc for reducing most of the grey-scale images displayed in [Figures 8](#) and [9](#), to Karen Teramura for preparing final versions of all of the figures, and to John Kormendy for his *TeX* macro, which was used to prepare preprints of this article. DBS was supported in part by [NASA](#) grants NAG5-1741 and NAGW-3938 and would like to acknowledge the hospitality of the [Service d'Astrophysique](#),

[Saclay](#), during extended visits while this article was being written.

[Next](#)

[Contents](#)

[Previous](#)



[Contents](#)

[Previous](#)

Literature Cited

1. Aaronson, M., Olszewski, E.W. [1984. *Nature* 309:414](#)
2. Allen, D.A., Roche, P.F., Norris, R.P. [1985. *MNRAS* 213:67P](#)
3. Antonucci, R.R.J., Miller, J.S. [1985. *Ap. J.* 297:621](#)
4. Antonucci, R.R.J., Olszewski, E.W. [1985. *Astron. J.* 90:2203](#)
5. Arp, H. [1966. *Ap. J. Suppl.* 14:1](#)
6. Armus, L., Heckman, T.M., Miley, G.K. [1987. *Astron. J.* 94:831](#)
7. Armus, L., Heckman, T.M., Miley, G.K. [1989. *Ap. J.* 347:727](#)
8. Armus, L., Heckman, T.M., Miley, G.K. [1990. *Ap. J.* 364:471](#)
9. Armus, L., Neugebauer, G., Soifer, B.T., Matthews, K. [1995a. *Astron. J.* 110:2610](#)
10. Armus, L., Shupe, D.L., Matthews, K., Soifer, B.T., Neugebauer, G. [1995b. *Ap. J.* 440:200](#)
11. Arnaud, M., Rothenflug, R., Boulade, O., Vigroux, L., Vagnioni-Flam, E. [1992. *Astron. Astrophys.* 254:49](#)
12. Ashby, M.L.N., Hacking, P.B., Houck, J.R., Soifer, B.T., Weisstein, E.W. [1996. *Ap. J.* 456:428](#)
13. Baan, W.A. [1985. *Nature* 315:26](#)
14. Baan, W.A. [1989. *Ap. J.* 338:804](#)
15. Baan, W.A. 1993. In *Astrophysical Masers*, ed. A.W. Clegg, G.E. Nedoluha, p. 73. New York: Springer Verlag
16. Baan, W.A., Haschick, A.D. [1984. *Ap. J.* 279:541](#)
17. Baan, W.A., Rhoads, J., Fisher, K., Altschuler, D.R., Haschick, A. [1992. *Ap. J. Lett.* 396:99](#)
18. Baan, W.A., van Gorkom, J., Schmelz, J.T., Mirabel, I.F. [1987. *Ap. J.* 313:102](#)
19. Baan, W.A., Wood, P.A.D., Haschick, A.D. [1982. *Ap. J. Lett.* 260:49](#)
20. Barnes, J.E. 1995. In *The Formation of Galaxies*, ed. C Muñoz-Tuñón, F Sanchez, p. 399. Cambridge: Cambridge University Press
21. Barnes, J.E., Hernquist, L. [1992. *Annu. Rev. Astron. Astrophys.* 30:705](#)
22. Barvainis, R., Alloin, D., Antonucci, R. [1989. *Ap. J. Lett.* 337:69](#)
23. Barvainis, R., Tacconi, L., Antonucci, R., Alloin, D., Coleman, P. [1994. *Nature* 371:586](#)
24. Barvainis, R., Antonucci, R., Hurt, T., Coleman, P., Reuter, H.P. [1995. *Ap. J. Lett.* 451:9](#)
25. Becklin, E.E., Matthews, K., Neugebauer, G., Wynn-Williams, G.C. [1973. *Ap. J. Lett.* 186:69](#)
26. Becklin, E.E., Wynn-Williams, C.G. 1987. In *Star Formation in Galaxies*, ed. C.J. Lonsdale-Persson, p. 643. Washington DC: US Govt. Print. Off.
27. Beichman, C.A., Soifer, B.T., Helou, G., Chester, T.J., Neugebauer, G., et al. [1986. *Ap. J. Lett.*](#)

[308:1](#)

28. Bhattacharya, D., The, L.-S., Kurfess, J.D., Clayton, D.D., Gehrels, N., Leising, M.D., et al. [1994. *Ap. J.* 437:173](#)
29. Bica, M.D., Kojoian G., Seal, J., Dickinson, D.F., Malkan, M.A. [1995. *Ap. J. Suppl.* 98:369](#)
30. Boller, T., Fink H., Schaeidt, S. [1994. *Astron. Astrophys.* 291:403](#)
31. Boller, T., Meurs, E.J.A., Brinkmann, W., Fink, H., Zimmermann, U., Adorf, H.M. [1992. *Astron. Astrophys.* 261:57](#)
32. Boller, T., Meurs, E.J.A., Dennefeld, M, Fink H. [1993. *Astrophys. Space Sci.* 205:43](#)
33. Bothun, G.D., Lonsdale, C.J., Rice, W.L. [1989. *Ap. J.* 341:129](#)
34. Braine, J., Combes, F., Casoli, F., Dupraz, C, Gérin, M., et al. [1993. *Astron. Astrophys. Suppl.* 97:887](#)
35. Broadhurst, T., Lehár, J. [1995. *Ap. J. Lett.* 450:41](#)
36. Brown, R.L., Vanden Bout, P.A. [1991. *Astron. J.* 102:1956](#)
37. Bryant, P. [1996. *High resolution observations of the molecular gas in luminous infrared galaxies.*](#)
PhD thesis, Calif. Inst. Tech., Pasadena
38. Burbidge, G.R., Stein, W.A. [1970. *Ap. J.* 160:573](#)
39. Bushouse, H.A. [1987. *Ap. J.* 320:49](#)
40. Bushouse, H.A., Lamb, S.A., Werner, M.W. [1988. *Ap. J.* 335:74](#)
41. Carico, D.P., Graham, J.R., Matthews, K., Wilson, T.D., Soifer, B.T., Neugebauer, G., Sanders, D.B. [1990. *Ap. J. Lett.* 349:39](#)
42. Casoli, F., Dupraz, C., Combes, F., Kazès, I. [1991. *Astron. Astrophys.* 251:1](#)
43. *Cataloged Galaxies and Quasars Observed in the IRAS Survey.* 1985. Prepared by C.J. Lonsdale, G. Helou, J.C. Good, W. Rice, Pasadena:JPL
44. Clements, D.L., Rowan-Robinson, M., Lawrence, A., Broadhurst, T., McMahon, R. [1992. *MNRAS* 256:35p](#)
45. Clements, D.L., Sutherland, W.J., McMahon, R.G., Saunders, W. [1996. *MNRAS* 279:477](#)
46. Clements, D.L., van der Werf, P.P., Krabbe, A., Blietz, M., Genzel, R., Ward, M.J. [1993. *MNRAS* 262:L23](#)
47. Condon, J.J., Anderson, M.L., Helou, G. [1991a. *Ap. J.* 376:95](#)
48. Condon, J.J., Dressel, L.L. [1978. *Ap. J.* 221:456](#)
49. Condon, J.J., Condon, M.A., Gisler, G., Puschell, J.J. [1982. *Ap. J.* 252:102](#)
50. Condon, J.J., Helou, G., Sanders, D.B., Soifer, B.T. [1990. *Ap. J. Suppl.* 73:359](#)
51. Condon, J.J., Huang, Z.-P., Yin, Q.F., Thuan, T.X. [1991b. *Ap. J.* 378:65](#)
52. Crawford, T., Marr, J., Partridge, B., Strauss, M.A. [1996. *Ap. J.* 460:225](#)
53. Cutri, R.M., Huchra, J.P., Low, F.J., Brown, R.B., Vanden Bout, P.A. [1994. *Ap. J. Lett.* 424:65](#)
54. Cutri, R.M., McAlary, C.W. [1985. *Ap. J.* 296:90](#)
55. David, L.P., Jones, C., Forman, W. [1992. *Ap. J.* 388:82](#)
56. de Grijp, M.H.K., Keel, W.C., Miley, G.K., Goudfrooij, P., Lub, J. [1992. *Astron. Astrophys. Suppl.* 96:389](#)

57. de Grijp, M.H.K., Miley, G.K., Lub, J., de Jong, T. [1985. *Nature* 314:240](#)
58. de Jong, T., Clegg, P.E., Soifer, B.T., Rowan-Robinson, M., Habing, H.J., et al. [1984. *Ap. J. Lett.* 278:67](#)
59. Dermer, C.D., Gehrels, N. [1995. *Ap. J.* 447:103](#)
60. Deutsch, L.K., Willner, S.P. [1986. *Ap. J. Lett.* 306:11](#)
61. Devereux, N., Taniguchi, Y., Sanders, D.B., Nakai, N., Young, J.S. [1994. *Astron. J.* 107:2006](#)
62. Devereux, N.A., Young, J.S. [1991. *Ap. J.* 371:515](#)
63. Dickey, J.M. [1986. *Ap. J.* 300:190](#)
64. Dickey, J.M., Salpeter, E.E. [1984. *Ap. J.* 284:461](#)
65. Downes, D., Radford, S.J.E., Greve, A., Thum, C., Solomon, P.M., Wink, J.E. [1992. *Ap. J. Lett.* 398:25](#)
66. Downes, D., Solomon, P.M., Radford, S.J.E. [1993. *Ap. J. Lett.* 414:13](#)
67. Downes, D., Solomon, P.M., Radford, S.J.E. [1995. *Ap. J. Lett.* 453:65](#)
68. Doyon, R., Wells, M., Wright, G.S., Joseph, R.D., Nadeau, D., James, P.A. [1994. *Ap. J. Lett.* 437:23](#)
69. Duc, P.A. [1995. *Genèse de galaxies naines dans les systèmes en interaction*. PhD thesis, Univ. Paris](#)
70. Duc, P.A., Mirabel, I.F. [1994. *Astron. Astrophys.* 289:83](#)
71. Dudley, C.C., Wynn-Williams, C.G. 1996. *Ap. J.* submitted
72. Dupraz, C., Casoli, F., Combes, F., Kazès, I. [1990. *Astron. Astrophys.* 228:L5](#)
73. Eales, S.A., Becklin, E.E., Hodapp, K.W., Simons, D.A., Wynn-Williams, C.G. [1990. *Ap. J.* 365:478](#)
74. Eales, S.A., Wynn-Williams, C.G., Duncan, W.D. [1989. *Ap. J.* 339:859](#)
75. Eisenhardt, P.R., Armus, L., Hogg, D.W., Soifer, B.T., Neugebauer, G., Werner, M.W. [1996. *Ap. J.* 461:72](#)
76. Elbaz, D., Arnaud, M., Cassé, M., Mirabel, I.F., Prantzos, N., Vangioni-Flam, E. [1992. *Astron. Astrophys.* 265:L29](#)
77. Elfhag, T., Booth, R.S., Hoglund, B., Johansson, L.E.B., Sandqvist, A. [1996. *Astron. Astrophys. Suppl.* 115:439](#)
78. Elmegreen, B.G. [1993. *Ap. J.* 411:170](#)
79. Elmegreen, B.G., Kaufman, M., Thomasson, M. [1993. *Ap. J.* 412:90](#)
80. Elston, R., Cornell, M.E., Lebofsky, M.J. [1985. *Ap. J.* 296:106](#)
81. Elston, R., McCarthy, P.J., Eisenhardt, P., Dickinson, M., Spinrad, H., et al. [1994. *Astron. J.* 107:910](#)
82. Elvis, M., Wilkes, B.J., McDowell, J.C., Green, R.F., Bechtold, J., et al. [1994 *Ap. J. Suppl.* 95:1](#)
83. Emerson, J.P., Clegg, P.E., Gee, G., Cunningham, C.T., Griffin, M.J., et al. [1984. *Nature* 311:237](#)
84. Evans, A.S. [1996. *The molecular gas content and ionization processes in distant powerful radio galaxies and hyperluminous infrared galaxies*. PhD thesis, Univ. Hawaii](#)
85. Evans, A.S., Sanders, D.B., Cutri, R., Radford, S.J.E., Solomon, P., et al. 1996a. *Ap. J.* submitted

86. Evans, A.S., Sanders, D.B., Mazzarella, J.M., Solomon, P.M., Downes, D., et al. [1996b. *Ap. J.* 457:658](#)
87. Fabbiano, G. [1988. *Ap. J.* 330:672](#)
88. Fabbiano, G., Heckman, T., Keel, W.C. [1990. *Ap. J.* 355:442](#)
89. Fairclough, J.H. [1986. *MNRAS* 219:1p](#)
90. Fisher, K.B., Huchra, J.P., Strauss, M.A., Davis, M., Yahil, A., Schlegel, D. [1995. *Ap. J. Suppl.* 100:69](#)
91. Fisher, K.B., Strauss, M.A., Davis, M., Yahil, A., Huchra, J.P. [1992. *Ap. J.* 389:188](#)
92. Fosbury, R.A.E., Wall, J.V. [1979. *MNRAS* 189:79](#)
93. Fritze-von Alvensleben, V., Gerhard, O.E. [1994. *Astron. Astrophys.* 285:775](#)
94. Frogel, J.A., Gillett, F.C., Terndrup, D.M., Vader, J.P. [1989. *Ap. J.* 343:672](#)
95. Gao, Y. [1996. *Dense molecular gas in galaxies and the evolution of luminous infrared galaxies.*](#) PhD thesis, SUNY at Stony Brook
96. Gherz, R.D., Sramek, R.A., Weedman, D.W. [1983. *Ap. J.* 267:551](#)
97. Goldader, J. [1995. *Near-infrared spectroscopy of luminous infrared galaxies.*](#) PhD thesis, Univ. Hawaii
98. Goldader, J., Joseph, R.D., Doyon, R., Sanders, D.B. [1995. *Ap. J.* 444:97](#)
99. Golombek, D., Miley, G.K., Neugebauer, G. [1988. *Astron. J.* 95:26](#)
100. Goodrich, R.W., Veilleux, S., Hill, G.J. [1994. *Ap. J.* 422:521](#)
101. Graham, J.R., Carico, D.P., Matthews, K., Neugebauer, G., Soifer, B.T., Wilson, T.D. [1990. *Ap. J. Lett.* 354:5](#)
102. Graham, J.R., Liu, M.C. [1995. *Ap. J. Lett.* 449:29](#)
103. Greenstein, J.L., Matthews, T.A. 1963. *Nature* 197:1041
104. Gregorich, D.T., Neugebauer, G., Soifer, B.T., Gunn, J.E., Herter, T.L. [1995. *Astron. J.* 110:259](#)
105. Griffiths, R.E., Padovani, P. [1990. *Ap. J.* 360:483](#)
106. Hacking, P.B., Condon, J.J., Houck, J.R. [1987. *Ap. J. Lett.* 316:15](#)
107. Hacking, P.B., Houck, J.R. [1987. *Ap. J. Suppl.* 63:311](#)
108. Harper, D.A., Low, F.J. [1973. *Ap. J. Lett.* 182:89](#)
109. Heckman, T.M. [1983. *Ap. J.* 268:628](#)
110. Heckman, T.M., Dahlem, M., Eales, S.A., Fabbiano, G., Weaver, K. [1996. *Ap. J.* 457:616](#)
111. Heckman, T.M., Armus, L., Miley, G.K. [1987. *Astron. J.* 93:276](#)
112. Heckman, T.M., Smith, E.P., Baum, S.A., van Breugel, W.J.M., Miley, G.K., et al. [1986. *Ap. J.* 311:526](#)
113. Heckman, T.M., Armus, L., Miley, G.K. [1990. *Ap. J. Suppl.* 74:833](#)
114. Heisler, C.A., Vader, J.P. [1994. *Astron. J.* 107:35](#)
115. Helou, G. [1986. *Ap. J. Lett.* 311:33](#)
116. Helou, G., Soifer, B.T., Rowan-Robinson, M. [1985. *Ap. J. Lett.* 298:7](#)
117. Hibbard, J.E., Guhathakurta, P., van Gorkom, J.H., Schweizer, F. [1994. *Astron. J.* 107:67](#)
118. Hibbard, J.E., van Gorkom, J.H. [1996. *Astron. J.* 111:655](#)

119. Hibbard, J.E., Yun, M.S. 1996. In *Cold Gas at High Redshift*, ed. M. Bremer, H. Rottgering, P. van der Werf, C. Carilli, p. 47. Dordrecht:Kluwer
120. Hill, G.J., Wynn-Williams, C.G., Becklin, E.E. [1987. *Ap. J. Lett.* 316:11](#)
121. Hines, D.C. [1991. *Ap. J. Lett.* 374:9](#)
122. Hines, D.C., Schmidt, G.D., Smith, P.S., Cutri, R.M., Low, F.J. [1995. *Ap. J. Lett.* 450:1](#)
123. Hines, D.C., Wills, B.J. [1993. *Ap. J.* 415:82](#)
124. Holtzman, J.A., Faber, S.M., Shaya, E.J., Lauer, T.R., Groth, E.J., et al. [1992. *Astron. J.* 103:691](#)
125. Houck, J.R., Schneider, D.P., Danielson, G.E., Beichman, C.A., Lonsdale, C.J., et al. [1985. *Ap. J. Lett.* 290:5](#)
126. Houck, J.R., Soifer, B.T., Neugebauer, G., Beichman, C.A., Aumann, H.H., et al. [1984. *Ap. J. Lett.* 278:63](#)
127. Hu, E.M., McMahon, R.G., Egami, E. [1996. *Ap. J. Lett.* 459:53](#)
128. Huchra, G. [1977. *Ap. J. Suppl.* 35:171](#)
129. Hummel, E. [1980. *Astron. Astrophys.* 89:L1](#)
130. Hunsberger, S.D., Charlton, J.C., Zaritsky, D. [1996. *Ap. J.* 462:50](#)
131. Hutchings, J.B., Neff, S.G. [1987. *Astron. J.* 93:14](#)
132. Impey, C., Gregorini, L. [1993. *Astron. J.* 105:853](#)
133. Impey, C., Neugebauer, G. [1988. *Astron. J.* 95:307](#)
134. *IRAS Point Source Catalog*, ver. 2. 1988. Washington:GPO (PSC)
135. Irwin, M., McMahon, R.G., Hazard, C. 1991. In *The Space Distribution of Quasars*, ed. D Crampton, p. 117. San Francisco: ASP
136. Isaak, K.G., McMahon, R.G., Hills, R.E., Withington, S. [1994. *MNRAS* 269:L28](#)
137. Isobe, T., Feigelson, E.D. [1992. *Ap. J. Suppl.* 79:197](#)
138. Iyengar, K.U.K., Verma, R.P. [1984. *Astron. Astrophys.* 139:64](#)
139. Jensen, J.B., Sanders, D.B., Wynn-Williams, C.G. 1996. *Ap. J.* submitted
140. Joseph, R.D., Meikle, W.P.S., Robertson, N.A., Wright, G.S. [1984a. *MNRAS* 209:111](#)
141. Joseph, R.D., Wright, G.S. [1985. *MNRAS* 214:87](#)
142. Joseph, R.D., Wright, G.S., Wade, R. [1984b. *Nature* 311:132](#)
143. Joy, M., Lester, D.F., Harvey, P.M., Frueh, M. [1986. *Ap. J.* 307:110](#)
144. Joy, M., Lester, D.F., Harvey, P.M., Telesco, C., Decher, R., et al. [1989. *Ap. J.* 339:100](#)
145. Kazès, I., Baan, W.A. [1991. *Astron. Astrophys.* 248:L15](#)
146. Kellermann, K.I., Sramek, R., Schmidt, M., Shaffer, D.B., Green, R. [1989. *Astron. J.* 98:1195](#)
147. Kennicutt, R.C., Keel, W.C., van der Hulst, J.M., Hummel, E., Roettiger, K.A. [1987. *Astron. J.* 93:1011](#)
148. Kennicutt, R.C., Kent, S.M. [1983. *Astron. J.* 88:1094](#)
149. Kim, D.C. [1995. *The IRAS 1 jy survey of ultraluminous infrared galaxies*](#). PhD thesis, Univ. Hawaii
150. Kim, D.C., Sanders, D.B. 1996. *Ap. J.* submitted
151. Kim, D.C., Sanders, D.B., Veilleux, S., Mazzarella, J.M., Soifer, B.T. [1995. *Ap. J. Suppl.* 98:129](#)
152. Kim, D.C., Veilleux, S., Sanders, D.B. 1996. *Ap. J.* submitted

153. Klaas, U., Elsasser, H. [1991. *Astron. Astrophys. Suppl.* 90:33](#)
154. Klaas, U., Elsasser, H. [1993. *Astron. Astrophys.* 280:76](#)
155. Kleinmann, D.E., Low, F.J. [1970a. *Ap. J. Lett.* 159:165](#)
156. Kleinmann, D.E., Low, F.J. [1970b. *Ap. J. Lett.* 161:203](#)
157. Kleinmann, S.G., Keel, W.C. 1987. In [*Star Formation in Galaxies*](#), ed. C.J. Lonsdale-Persson, p. 559. Washington, DC: US Govt. Print. Off.
158. Knapp, G.R., Bies, W.E., van Gorkom, J.H. [1990. *Astron. J.* 99:476](#)
159. Knapp, G.R., Guhathakurta, P., Kim, D.W., Jura, M. [1989. *Ap. J. Suppl.* 70:329](#)
160. Kormendy, J., Sanders, D.B. [1992. *Ap. J. Lett.* 390:53](#)
161. Larson, R.B., Tinsley, B.M. [1978. *Ap. J.* 219:46](#)
162. Lawrence, A., Rowan-Robinson, M., Leech, K., Jones, D.H.P., Wall, J.V. [1989. *MNRAS* 240:329](#)
163. Lawrence, A., Rowan-Robinson, M., Saunders, W., Parry, I.R., Xiaoyang, X., et al. 1996. *MNRAS* In press
164. Lawrence, A., Walker, D., Rowan-Robinson, M., Leech, K.J., Penston, M.V. [1986. *MNRAS* 219:687](#)
165. Lebofsky, M.J., Rieke, G.H. [1979. *Ap. J.* 229:111](#)
166. Leech, K.J., Rowan-Robinson, M., Lawrence, A., Hughes, J.D. [1994. *MNRAS* 267:253](#)
167. Lester, D.F., Joy, M., Harvey, P.M., Ellis, H.B., Parmar, P.S. [1987. *Ap. J.* 321:755](#)
168. Loewenstein, M., Mushotzky, R.F. [1996. *Ap. J.* 466:695](#)
169. Longmore, A.J., Hawarden, T.G., Cannon, R.D., Allen D.A., Mebold, U., et al. [1979. *MNRAS* 188:285](#)
170. Lonsdale, C.J., Diamond, P.J., Smith, H.E., Lonsdale, C.J. [1994. *Nature* 370:117](#)
171. Lonsdale, C.J., Hacking, P. [1989. *Ap. J.* 339:712](#)
172. Lonsdale, C.J., Hacking, P., Conrow, T.P., Rowan-Robinson, M. [1990. *Ap. J.* 358:60](#)
173. Lonsdale, C.J., Persson, S.E., Matthews, K. [1984. *Ap. J.* 287:95](#)
174. Lonsdale, C.J., Smith, H.E., Lonsdale, C.J. [1993 *Ap. J. Lett.* 405:9](#)
175. Low, F.J., Huchra, J.P., Kleinmann, S.G., Cutri, R.M. [1988. *Ap. J. Lett.* 327:41](#)
176. Low, F.J., Kleinmann, D.E. [1968. *Astron. J.* 73:868](#)
177. MacKenty, J.W., Stockton, A. [1984. *Ap. J.* 283:64](#)
178. Martin, J.M., Bottinelli, L., Dennefeld, M., Gouguenheim, L., Le Squeren, A.M. [1988. *Astron. Astrophys.* 201:L13](#)
179. Martin, J.M., Bottinelli, L., Dennefeld, M., Gouguenheim, L., Le Squeren, A.-M. 1991. In [*Dynamics of Galaxies and their Molecular Cloud Distributions*](#), ed. F Combes, F Casoli, p. 447. Dordrecht:Reidel
180. Matthews, K., Neugebauer, G., McGill, J., Soifer, B.T. [1987. *Astron. J.* 94:297](#)
181. Matthews, K., Soifer, B.T., Nelson, J., Boesgaard, H., Graham, J.R., et al. [1994. *Ap. J. Lett.* 420:13](#)
182. Matthews, T.A., Sandage, A.R. [1963. *Ap. J.* 138:30](#)
183. Mauersberger, R., Henkel, C. [1993. *Astron. Gesellschaft. Rev. Mod. Astron.* 6:69](#)
184. Mazzarella, J.M., Graham, J.R., Sanders, D.B., Djorgovski, G. [1993. *Ap. J.* 409:170](#)

185. Mazzarella, J.M., Balzano, V.A. [1986. *Ap. J. Suppl.* 62:751](#)
186. Mazzarella, J.M., Bothun, G.D., Boroson, T. [1991. *Astron. J.* 101:2034](#)
187. McMahon, R.G., Omont, A., Bergeron, J., Kreysa, E., Haslam, C.G.T. [1994. *MNRAS* 267:L9](#)
188. Melnick, J., Mirabel, I.F. [1990. *Astron. Astrophys.* 231:L19](#)
189. Meurer, G.R. [1995. *Nature* 375:742](#)
190. Meurer, G.R., Heckman, T.M., Leitherer, C., Kinney, A., Robert, C., Garnett, D.R. [1995. *Astron. J.* 110:2665](#)
191. Mihos, J.C., Hernquist, L. [1994. *Ap. J. Lett.* 431:9](#)
192. Miles, J.W., Houck, J.R., Hayward, T.L., Ashby M.L.N. [1996. *Ap. J.* 465:191](#)
193. Miley, G., Neugebauer, G., Clegg, P.E., Harris S., Rowan-Robinson M., et al. [1984. *Ap. J. Lett.* 278:79](#)
194. Miley, G.K., Neugebauer, G., Soifer, B.T. [1985. *Ap. J. Lett.* 293:11](#)
195. Mirabel, I.F. [1982. *Ap. J.* 260:75](#)
196. Mirabel, I.F. [1989. *Ap. J. Lett.* 340:13](#)
197. Mirabel, I.F., Booth, R.S., Garay, G., Johansson, L.E.B., Sanders, D.B. [1990. *Astron. Astrophys.* 236:327](#)
198. Mirabel, I.F., Dottori, H., Lutz, D. [1992. *Astron. Astrophys.* 256:L19](#)
199. Mirabel, I.F., Duc, P.A., Dottori, H. 1995. In *Dwarf Galaxies*, ed. G Meylan, P Prugniel, p. 371. Garching bei Munchen:ESO
200. Mirabel, I.F., Kazès, I., Sanders, D.B. [1988. *Ap. J. Lett.* 324:59](#)
201. Mirabel, I.F., Lutz, D., Maza, J. [1991. *Astron. Astrophys.* 243:367](#)
202. Mirabel, I.F., Sanders, D.B. [1987. *Ap. J.* 322:688](#)
203. Mirabel, I.F., Sanders, D.B. [1988. *Ap. J.* 335:104](#)
204. Mirabel, I.F., Sanders, D.B. [1989. *Ap. J. Lett.* 340:53](#)
205. Mirabel, I.F., Sanders, D.B., Kazès, I. [1989. *Ap. J. Lett.* 340:9](#)
206. Miyoshi, M., Moran, J., Herrnstein, J., Greenhill, L., Nakai, N., et al. [1995. *Nature* 373:127](#)
207. Mobasher, B., Sharples, R.M., Ellis, R.S. [1993. *MNRAS* 263:560](#)
208. Montgomery, A.S., Cohen, R.J. [1992. *MNRAS* 254:23p](#)
209. Moore, B., Katz, N., Lake, G., Dressler, A., Oemler, A. [1996. *Nature* 379:613](#)
210. Moshir, M., Kopman, G., Conrow, J., McCallon, H., Hacking, P., et al. 1992. *Explanatory Supplement to the IRAS Faint Source Survey, Version 2*, JPL D-10015 8/92, Pasadena: JPL
211. Murphy, T.W., Armus, L., Matthews, K., Soifer, B.T., Mazzarella, J.M., et al. [1996. *Astron. J.* 111:1025](#)
212. Neugebauer, G., Becklin, E.E., Hyland, A.R. [1971. *Annu. Rev. Astron. Astrophys.* 9:67](#)
213. Neugebauer, G., Becklin, E.E., Oke, J.B., Searle, L. [1976. *Ap. J.* 205:29](#)
214. Neugebauer, G., Habing, H.J., van Duinen, R., Aumann, H.H., Baud, B, et al. [1984 *Ap. J. Lett.* 278:1](#)
215. Neugebauer, G., Soifer, B.T., Miley, G.K. [1985. *Ap. J. Lett.* 295:27](#)
216. Neugebauer, G., Soifer, B.T., Miley, G.K., Clegg, P.E. [1986. *Ap. J.* 308:815](#)

217. Ohta, K., Yamada, T., Nakanishi, K., Kohno, K., Akiyama, M., Kawabe, R. [1996. *Nature* 382:426](#)
218. Okumura, S.K., Kawabe, R., Ishiguro, M., Kasuga, T., Morita, K.I., Ishizuki S. 1991. In [*Dynamics of Galaxies and Their Molecular Cloud Distributions*](#), ed. F Combes, F Casoli, p. 425. Dordrecht:Reidel
219. Oliver, S., Broadhurst, T., Rowan-Robinson, M., Saunders, W., Lawrence, A., et al. 1995. In [*Wide-Field Spectroscopy and the Distant Universe*](#), ed. SJ Maddox, A Aragon-Salamanca, p. 264. Singapore:World Scientific
220. Oliver, S., Rowan-Robinson, M., Broadhurst, T.J., McMahon, R.G., Saunders, W., et al. [1996. *MNRAS* 280:673](#)
221. Omont, A., McMahon, R.G., Cox, P., Kreysa, E., Bergeron, J., et al. 1996a. *Astron. Astrophys.* In press
222. Omont, A., Petitjean, P., Guilloteau, S., McMahon, R.G., Solomon, P.M., Pécontal, E. [1996b. *Nature* 382:428](#)
223. Osterbrock, D.E., DeRobertis, M.M. [1985. *Publ. Astron. Soc. Pac.* 97:1129](#)
224. Perault, M. [1987. *Structure et evolution des nuages moleculaires*](#). PhD thesis, Univ. Paris
225. Radford, S.J.E. 1994. In [*The Cold Universe*](#), ed. T Montmerle, CJ Lada, IF Mirabel, J Tran Thanh Van, p. 369. Gif-sur-Yvette:Ed Frontieres
226. Radford, S.J.E., Downes, D., Solomon, P.M., Barrett, J., Sage, L.J. [1996. *Astron. J.* 111:1021](#)
227. Radford, S.J.E., Solomon, P.M., Downes, D. [1991. *Ap. J. Lett.* 368:15](#)
228. Read, A.M., Ponman, T.J., Wolstecroft, R.D. [1995. *MNRAS* 277:397](#)
229. Rees, M.J., Silk, J.I., Werner, M.W., Wickramasinghe, N.C. 1969. *Nature* 223:37
230. Rieke, G.H. [1978. *Ap. J.* 226:550](#)
231. Rieke, G.H. [1988. *Ap. J. Lett.* 331:5](#)
232. Rieke, G.H., Cutri, R., Black, J.H., Kailey, W.F., McAlary, C.W., Lebofsky, M.J., Elston, R. [1985. *Ap. J.* 290:116](#)
233. Rieke, G.H., Lebofsky, M.J. [1978. *Ap. J. Lett.* 220:37](#)
234. Rieke, G.H., Lebofsky, M.J. [1979. *Annu. Rev. Astron. Astrophys.* 17:477](#)
235. Rieke, G.H., Lebofsky, M.J. [1986. *Ap. J.* 304:326](#)
236. Rieke, G.H., Low, F.J. [1972. *Ap. J. Lett.* 176:95](#)
237. Rieke, G.H., Low, F.J. [1975. *Ap. J. Lett.* 200:67](#)
238. Rigopoulou, D., Lawrence, A., Rowan-Robinson, M. [1996a. *MNRAS* 278:1049](#)
239. Rigopoulou, D., Lawrence, A., White, G.J., Rowan-Robinson, M., Church, S.E. [1996b. *Astron. Astrophys.* 305:747](#)
240. Rowan-Robinson, M. [1986. *MNRAS* 219:737](#)
241. Rowan-Robinson, M., Broadhurst, T., Lawrence, A., McMahon, R.G., Lonsdale, C.J., et al. [1991. *Nature* 351:719](#)
242. Rowan-Robinson, M., Clegg, P.E., Beichman, C.A., Neugebauer, G., Soifer, B.T., et al. [1984. *Ap. J. Lett.* 278:7](#)
243. Rowan-Robinson, M., Efstathiou, A. [1993. *MNRAS* 263:675](#)
244. Rush, B., Malkan, M.A., Spinoglio, L. [1993. *Ap. J. Suppl.* 89:1](#)

245. Sage, L.J., Solomon P.M. [1987. *Ap. J. Lett.* 321:103](#)
246. Sanders, D.B. 1992. In [Relationships Between Active Galactic Nuclei and Starburst Galaxies](#), ed. A Filippenko, p. 303. San Francisco:PASP
247. Sanders, D.B., Egami, E., Lipari, S., Mirabel, I.F., Soifer, B.T. [1995. *Astron. J.* 110:1993](#)
248. Sanders, D.B., Mazzarella, J.M., Jensen, J., Wynn-Williams, C.G., Hodapp, K.W. 1996b. *Ap. J. Suppl.* submitted
249. Sanders, D.B., Mirabel, I.F. [1985. *Ap. J. Lett.* 298:31](#)
250. Sanders, D.B., Phinney, E.S., Neugebauer, G., Soifer, B.T., Matthews, K. [1989a. *Ap. J.* 347:29](#)
251. Sanders, D.B., Sargent, A.I., Scoville, N.Z., Phillips, T.G. 1990. In [Submillimeter Astronomy](#), ed. GD Watt, A Webster, p. 213. Dordrecht:Kluwer
252. Sanders, D.B., Scoville, N.Z., Soifer, B.T. [1988c. *Ap. J. Lett.* 335:1](#)
253. Sanders, D.B., Scoville, N.Z., Soifer, B.T. [1988d. *Science* 239:625](#)
254. Sanders, D.B., Scoville, N.Z., Soifer, B.T. [1991. *Ap. J.* 370:158](#)
255. Sanders, D.B., Scoville, N.Z., Zensus, A., Soifer, B.T., Wilson, T.L., et al. [1989b. *Astron. Astrophys.* 213:L5](#)
256. Sanders, D.B., Soifer, B.T., Elias, J.H., Madore, B.F., Matthews, K., et al. [1988a. *Ap. J.* 325:74](#)
257. Sanders, D.B., Soifer, B.T., Elias, J.H., Neugebauer, G., Matthews, K. [1988b. *Ap. J. Lett.* 328:35](#)
258. Sanders, D.B., Mazzarella, J.M., Surace, J., Egami, E., Kim, D.C., et al. 1996a, *Ap. J. Suppl.* submitted
259. Sanders, D.B., Young, J.S., Scoville, N.Z., Soifer, B.T., Danielson, G.E. [1987b. *Ap. J. Lett.* 312:5](#)
260. Saunders, W., Rowan-Robinson, M., Lawrence, A., Efstathiou, G., Kaiser, N., et al. [1990. *MNRAS* 242:318](#)
261. Schechter, P. [1976. *Ap. J.* 203:297](#)
262. Schmidt, M., Green, R.F. [1983. *Ap. J.* 269:352](#)
263. Schweizer, F. 1978. In [Structure and Properties of Nearby Galaxies](#), ed. E.M. Berkhuysen, R. Wielebinski, p. 279. Dordrecht:Reidel
264. Schweizer, F. [1982. *Ap. J.* 252:455](#)
265. Scoville, N.Z., Padin, S., Sanders, D.B., Soifer, B.T., Yun, M.S. [1993. *Ap. J. Lett.* 415:75](#)
266. Scoville, N.Z., Sanders, D.B. 1987. In [Interstellar Processes](#), ed. H. Thronson, D. Hollenbach, p. 21. Dordrecht: Reidel
267. Scoville, N.Z., Sargent, A.Z., Sanders, D.B., Soifer, B.T. [1991. *Ap. J. Lett.* 366:5](#)
268. Scoville, N.Z., Yun, M.S., Brown, R.L., Vanden Bout, P.A. [1995. *Ap. J. Lett.* 449:109](#)
269. Smith, B.J., Kleinmann, S.G., Huchra, J.P., Low, F.J. [1987. *Ap. J.* 318:161](#)
270. Soifer, B.T., Boehmer, L., Neugebauer, G., Sanders D.B. [1989. *Astron. J.* 98:766](#)
271. Soifer, B.T., Cohen, J.G., Armus, L., Matthews, K., Neugebauer, G., Oke J.B. [1995. *Ap. J. Lett.* 443:65](#)
272. Soifer, B.T., Helou, G., Lonsdale, C.J., Neugebauer G., Hacking P., et al. [1984b. *Ap. J. Lett.* 283:1](#)
273. Soifer, B.T., Houck, J.R., Neugebauer, G. [1987a. *Annu. Rev. Astron. Astrophys.* 25:187](#)
274. Soifer, B.T., Neugebauer, G. [1991. *Astron. J.* 101:354](#)
275. Soifer, B.T., Neugebauer, G., Matthews, K., Lawrence, C., Mazzarella, J. [1992. *Ap. J. Lett.* 399:55](#)

276. Soifer, B.T., Rowan-Robinson, M., Houck, J.R., de Jong, T., Neugebauer, G., et al. [1984a. *Ap. J. Lett.* 278:71](#)
277. Soifer, B.T., Sanders, D.B., Madore, B.F., Neugebauer, G., Danielson, G.E., et al. [1987b. *Ap. J.* 320:238](#)
278. Soifer, B.T., Sanders, D.B., Neugebauer, G., Danielson, G.E., Lonsdale, C.J., et al. [1986. *Ap. J. Lett.* 303:41](#)
279. Solomon, P.M., Downes, D., Radford, S.J.E. [1992a. *Ap. J. Lett.* 387:55](#)
280. Solomon, P.M., Downes, D., Radford, S.J.E. [1992b. *Ap. J. Lett.* 398:29](#)
281. Solomon, P.M., Downes, D., Radford, S.J.E., Barrett J.W. 1996. *Ap. J.* In press
282. Solomon, P.M., Radford, S.J.E., Downes, D. [1992c. *Nature* 356:318](#)
283. Spinoglio, L., Malkan, M.A. [1989. *Ap. J.* 342:83](#)
284. Stanford, S.A., Bushouse, H.A. [1991. *Ap. J.* 371:92](#)
285. Stanford, S.A., Sargent, A.I., Sanders, D.B., Scoville, N.Z. [1990. *Ap. J.* 349:492](#)
286. Staveley-Smith, L., Cohen, R.J., Chapman, J.M., Pointon, L., Unger, S.W. [1987. *MNRAS* 226:689](#)
287. Stein, W.A. [1995. *Astron. J.* 110:1019](#)
288. Stein, W.A., Gillett, F.C., Merrill, K.M. [1974. *Ap. J.* 187:213](#)
289. Stockton, A., Ridgway, S.E. [1991. *Astron. J.* 102:488](#)
290. Strauss, M.A., Huchra, J.P. [1988. *Astron. J.* 95:1602](#)
291. Strauss, M.A., Huchra, J.P., Davis, M., Yahil, A., Fisher, K.B., Tonry, J. [1992. *Ap. J. Suppl.* 83:29](#)
292. Sulentic, J.W. [1989. *Astron. J.* 98:2066](#)
293. Tacconi, L.J., Genzel, R., Bleitz, M., Cameron, M., Harris, A.I., Madden, S. [1994. *Ap. J. Lett.* 426:77](#)
294. Taniguchi, Y., Wada, K. [1996. *Ap. J.* 469:581](#)
295. Telesco, C.M. [1988. *Annu. Rev. Astron. Astrophys.* 26:343](#)
296. Telesco, C.M., Harper, D.A. [1980. *Ap. J.* 235:392](#)
297. Terlevich, R.J., Boyle, B.J. [1993. *MNRAS* 262:491](#)
298. Tinney, C.G., Scoville, N.Z., Sanders, D.B., Soifer, B.T. [1990. *Ap. J.* 362:473](#)
299. Toomre, A. 1977. In *The Evolution of Galaxies and Stellar Populations*, ed. BM Tinsley, RB Larson, p. 401. New Haven, CT:Yale Univ. Obs.
300. Toomre, A., Toomre, J. [1972. *Ap. J.* 178:623](#)
301. Trentham, N. [1995. *MNRAS* 277:616](#)
302. Ueno, S., Mushotsky, R.F., Koyama, K., Iwasawa, K., Awaki, H., Hayashi, I. [1994 *Publ. Astron. Soc. Japan* 46:L71](#)
303. Ulvestad, J.S., Wilson, A.S. [1989. *Ap. J.* 343:659](#)
304. Vacca, W.D. 1996. In *The Interplay Between Massive Star Formation, the ISM, and Galaxy Evolution*, ed. D. Knuth, B. Guiderdoni, M. Heydari-Malayeri, T. Thuan, p. 321. Paris: Ed.Frontieres
305. Vader, J.P., Frogel, J.A., Terndrup, D.M., Heisler, C.A. [1993. *Astron. J.* 106:1743](#)
306. Vader, J.P., Simon, M. [1987a. *Nature* 327:304](#)

307. Vader, J.P., Simon, M. [1987b. *Astron. J.* 94:854](#)
308. van den Bergh, S. 1990. In *Dynamics and Interactions of Galaxies*, ed. R Wielen, p. 492. Dordrecht:Reidel
309. van den Bergh, S. [1995a. *Nature* 374:215](#)
310. van den Bergh, S. [1995b. *Ap. J.* 450:27](#)
311. van den Broek, A.C. [1990. *A study of extreme IRAS galaxies*. PhD thesis, Univ. Groningen](#)
312. van der Kruit, P.C. [1971. *Astron. Astrophys.* 15:110](#)
313. Veilleux, S., Cecil, G., Bland-Hawthorn, J., Tully, R.B., Filippenko, A.V., Sargent, W.L.W. [1994. *Ap. J.* 433:48](#)
314. Veilleux, S., Kim, D.-C., Sanders, D.B. 1996. *Ap. J.* submitted
315. Veilleux, S., Kim, D.-C., Sanders, D.B., Mazzarella, J.M., Soifer, B.T. [1995. *Ap. J. Suppl.* 98:171](#)
316. Veilleux, S., Osterbrock, D.E. [1987. *Ap. J. Suppl.* 63:295](#)
317. Vorontsov-Velyaminov, B.A. [1959. *Atlas and Catalog of Interacting Galaxies, Vol I*, Moscow: Sternberg Inst., Moscow State Univ.](#)
318. Wang, Z., Schweizer, F., Scoville, N.Z. [1992. *Ap. J.* 396:510](#)
319. Whitmore, B.C., Schweitzer, F. [1995. *Astron. J.* 109:960](#)
320. Whitmore, B.C., Schweitzer, F., Leitherer, C., Borne, K., Robert, C. [1993. *Astron. J.* 106:1354](#)
321. Wright, G.S., James, P.A., Joseph, RD, McLean, IS. [1990. *Nature* 344:417](#)
322. Wright, G.S., Joseph, R.D., Meikle, W.P.S. [1984. *Nature* 309:430](#)
323. Wunderlich, E., Klein, U., Wielebinski, R. [1987. *Astron. Astrophys. Suppl.* 69:487](#)
324. Xu, C., Lisenfeld, U., Völk H.J. [1994. *Astron. Astrophys.* 285:19](#)
325. Young, E.T., Neugebauer, G., Kopan, E.L., Benson, R.D., Conrow, T.P., et al. 1986. *A Users Guide to the IRAS Pointed Observation Products*, Pasadena: JPL
326. Young, J.S., Kenney, J.D., Lord, S., Schloerb, F.P. [1984. *Ap. J. Lett.* 287:65](#)
327. Young, J.S., Kenney, J.D., Tacconi, L., Clausen, M.J., Huang, Y.L., et al. [1986b *Ap. J. Lett.* 311:17](#)
328. Young, J.S., Schloerb, F.P., Kenney, J., Lord, S. [1986a. *Ap. J.* 304:443](#)
329. Young, J.S., Scoville, N.Z. [1991. *Annu. Rev. Astron. Astrophys.* 29:581](#)
330. Young, J.S., Xie, S., Tacconi, L., Knezek, P., Viscuso, P., et al. [1995. *Ap. J. Suppl.* 98:219](#)
331. Zwicky, F. 1956. *Ergeb. Exakten Naturwiss.* 29:34
332. Zwicky, F., Zwicky, M.A. [1971. *Catalog of Selected Galaxies and Post-Eruptive Galaxies*. Zurich: Offsetdruck L. Speich](#)

[Contents](#)[Previous](#)